single bond.[10] In compounds with the Mo_2^{6+} core, the observed terminal Mo-O distance is 1.80-1.96 Å and is a result of the π-bonding component of the Mo-O bond. In our compound, the molybdenum atom, as in other Mo_2^{4+} core complexes, has no vacant d orbitals that can accept π-electron density from the pentafluorophenoxide ligands. A weak Mo-O π bond is possible by the mixing of the oxygen π orbitals with the δ^* and π^* orbitals of the Mo-Mo bond. The latter tends to shorten the Mo-O bond and lengthen the Mo-Mo bond, and indeed, that seems to be the case for compounds **2** and **4** as listed in Table I. Our species appears to contain only a single Mo-O bond without any Mo-O π component. This was expected, since the pentafluorophenoxide ligand has highly electron-withdrawing fluorides, which decrease the amount of electron density available to the oxygen atom's π orbitals.

Conclusions

This report adds two important pieces of information to the literature. First, the coordinatively saturated $Mo_2(CH_3)_4(PMe_3)_4$ species are reactive toward alcoholic species and allow a direct synthetic route to $Mo_2(OC_6F_5)_4(PMe_3)_4$. Second, complex **1** represents the first centrosymmetric [*cis*-$Mo(OR)_2(L)_2]_2$ species that contains all monodentate ligands.

Acknowledgment. We thank the National Science Foundation for support.

Supplementary Material Available: Tables of complete bond distances and angles and general displacement parameter expressions (5 pages); a table of observed and calculated structure factors (16 pages). Ordering information is given on any current masthead page.

Contribution from the Department of Chemistry,
The University of Michigan, Ann Arbor, Michigan 48109-1055

Studies of the Reactivity of Binary Thio- and Tertiary Oxothiomolybdates toward Electrophiles. Reactions with Dicarbomethoxyacetylene and the Synthesis and Structures of the $[Et_4N]_2[MoO(L)_2]$, *anti*-$[Et_4N]_2[Mo_2O_2S_2(L)_2]$, *syn*-$[Ph_4P]_2[Mo_2O_2S_2(L)_2]\cdot 2DMF$, $[Ph_4P]_2[Mo(L)_3]\cdot DMF\cdot C_6H_6$, and $[Ph_4P]_2[Mo_2S_2(L)_4]\cdot 2CH_2Cl_2$ Complexes (L = 1,2-Dicarbomethoxy-1,2-ethylenedithiolate)

D. Coucouvanis,* A. Hadjikyriacou, A. Toupadakis, Sang-Man Koo, O. Ileperuma, M. Draganjac, and A. Salifoglou

Received July 6, 1990

The reactions of various thio- or oxothiomolybdates with the activated alkyne dicarbomethoxyacetylene, DMA, are described. The syntheses of the diamagnetic $[Et_4N]_2[MoO(L)_2]$ (I), *anti*-$[Et_4N]_2[Mo_2O_2S_2(L)_2]$ (II), *syn*-$[Ph_4P]_2[Mo_2O_2S_2(L)_2]\cdot 2DMF$ (III), $[Ph_4P]_2[Mo(L)_3]\cdot DMF\cdot C_6H_6$ (IV), and $[Ph_4P]_2[Mo_2S_2(L)_4]\cdot 2CH_2Cl_2$ (V) complexes (L = 1,2-dicarbomethoxy-1,2-ethylenedithiolate, DMAD) are accomplished in reactions of DMA with $(Et_4N)_2[MoO(S_4)_2]$, $(Et_4N)_2[Mo_2O_2S_9]$, $(Ph_4P)_2[Mo_2OS_7]$, $(Ph_4P)_2[MoS(S_4)_2]$, and $(Ph_4P)_2[Mo_2S_{10}/S_{12}]$, respectively. It is proposed that these reactions proceed by electrophilic attack of DMA on either Mo=S or Mo-S_2 with subsequent DMA insertion into these chromophores. The unstable vinyl sulfide or vinyl disulfide intermediates are converted to the final dithiolene products either thermally or by a sulfur-catalyzed pathway. The compounds I-V crystalize in the space groups $P2_1/c$, $P\bar{1}$, $P\bar{1}$, $C2/c$, and $P\bar{1}$, respectively. The cell dimensions are a = 17.664 (4) Å, b = 9.979 (2) Å, c = 21.363 (4) Å, and β = 100.5 (2)° for I, a = 9.004 (2) Å, b = 8.975 (3) Å, c = 13.904 (2) Å, α = 90.53 (2)°, β = 102.04 (1)°, and γ = 112.11 (2)° for II, a = 12.919 (4) Å, b = 14.863 (6) Å, c = 18.844 (6) Å, α = 95.86 (3)°, β = 102.61 (2)°, and γ = 93.74 (3)° for III, a = 22.907 (14) Å, b = 14.619 (9) Å, c = 43.746 (21) Å, and β = 95.34 (5)° for IV, and a = 12.778 (2) Å, b = 13.616 (3) Å, c = 13.898 (3) Å, α = 105.62 (2)°, β = 98.80 (1)°, and γ = 110.10 (1) for V. The data for all structures were obtained on an automatic diffractometer employing Mo Kα radiation. Full-matrix refinement of 393 parameters on 2704 data for I, 217 parameters on 1774 data for II, 775 parameters on 6350 data for III, 389 parameters on 2637 data for IV, and 313 parameters on 2412 data for V gave final R_w values of 0.050, 0.024, 0.044, 0.077, and 0.066, respectively. The structure of I shows the Mo^{IV} coordinated by a terminal oxo ligand and two bidentate DMA ligands in the equatorial plane of the distorted square-pyramidal $Mo^{IV}(O)(S_4)$ core unit (Mo=O = 1.686 (6) Å; Mo-S_{eq} = 2.380 (4) Å). The structures of the *anti*- and *syn*-$[Mo_2O_2(\mu_2\text{-}S)_2]^{2+}$ units in II and III have idealized C_{2h} and C_{2v} geometry, respectively. Each unit is coordinated by two DMAD bidentate ligands. The $Mo^V(O)(S_4)$ subunits are distorted square pyramidal with a terminal oxo ligand and the DMAD and μ_2-S ligands occupying the equatorial planes. Adjacent pyramids share the bridging S ligands as common equatorial sites (for II, Mo-Mo = 2.904 (1) Å, Mo=O = 1.684 (2) Å, Mo-S_b = 2.328 Å, Mo-S_L = 2.419 Å, Mo-S_b-Mo = 77.13 (1)°, and S_b-Mo-S_b = 102.91 (1)°; for III, Mo-Mo = 2.853 (1) Å, Mo=O = 1.675 (2) Å, Mo-S_b = 2.331 (3) Å, Mo-S_L = 2.425 (8) Å, Mo-S_b-Mo = 75.5 (1)°, and S_b-Mo-S_b = 100.9 (1)°). The structure of IV shows the Mo(IV) coordinated by three bidentate DMAD ligands and contains the slightly distorted trigonal prismatic $[Mo^{IV}(S)_6]$ core (Mo-S_L = 2.393 Å). The structure of the centrosymmetric anion in V contains two edge-sharing distorted octahedral $[Mo^V(S)_6]$ units that share the bridging S ligands. The Mo^V in each of these subunits, in addition to the two bridging sulfides, is coordinated by two bidentate DMAD ligands (Mo-Mo = 2.938 Å, Mo-S_b = 2.321 Å, Mo-S_L = 2.383, 2.459 Å; Mo-S_b-Mo = 78.6 (1)°, S_b-Mo-S_b = 101.4 (1)°). The different Mo-S_L bonds in V are attributed to a significant trans effect of the bridging ligands. The spectroscopic and electrochemical properties of these complexes as well as a discussion of the reactivity characteristics of the various Mo-centered functional groups are discussed.

Introduction

In the last decade our understanding of synthetic and structural aspects in the chemistry of the binary Mo/S and tertiary Mo/S/O complexes has reached a relatively advanced level. As a result of extensive synthetic and crystallographic studies in various laboratories, nearly complete series of the $[(L)Mo(E)(\mu\text{-}S)_2Mo(E')(L')]^{2-}$ anions (Figure 1) (E = E' = S: L = L' = S;[1] L = S, L' = S_2;[1] L = L' = S_2;[2] L = S, L' = S_4;[1] L = S_2, L' = S_4;[3]

(1) Hadjikyriacou, A. I.; Coucouvanis, D. *Inorg. Chem.* **1987**, *26*, 2400.

0020-1669/91/1330-0754$02.50/0

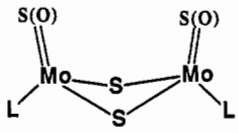

Figure 1. Schematic structure of the $[(L)(Mo(E)(\mu\text{-}S)_2Mo(E')(L')]^{n-}$ anions.

L = L′ = S_4;[3a,4] L = S, L′ = MoS_4.[5] E = O, E′ = S: L = S, L′ = S_2;[6] L = L′ = S_2;[6,7] L = S, L = S_4;[6] L = S_2, L′ = S_4;[6] L′ = S, L = MoS_4.[8] E = E′ = O: L = L′ = S_2;[9] L = S, L′ = S_4;[10] L = S_2, L′ = S_4;[11] L = L′ = S_4;[12] L = S_2, L′ = MoS_4;[13] L = S, L′ = MoS_4[13d]) are now available.

In addition the Mo(VI)-containing complexes $[Mo_2O_2S_9]^{2-}$, $[Mo_4O_4S_{18}]^{2-}$, and $[Mo_2O(S_2)_2(C_2O_3S)]^{2-}$ have been synthesized and structurally characterized[14a-d] and the synthesis of the $[Mo_2S_2S_9]^{2-}$ complex has been reported.[14e] Other monomeric or trimeric complexes known include the $([MoO_nS_{4-n}]^{2-}$ anions,[15] the $[(E)Mo(S_4)_2]^{2-}$ anions,[3] (E = S, O), and $(Mo_3S_{13})^{2-}$.[16]

As a consequence of facile intramolecular electron-transfer processes, which very likely derive from a close matching of the S 3p and Mo 4d orbital energies,[17] certain of the molybdothioanions display a diversity in structural isomerism. The ground states of electron-redistribution isomers of isoelectronic complexes at times are close enough in energy so that minor perturbations (crystal packing forces, solvent dielectrics, ion pairing) are sufficient to preferentially stabilize one isomer over another. A remarkable example of such an event is the existence, isolation, and structural characterization of the $[Mo^V_2(S_2)_6]^{2-}$[19] and $[(S_4)(Mo^V(S)(\mu\text{-}S)_2Mo^V(S)(S_4)]^{2-}$[3a,4] anions. The former, isolated from aqueous solution as a NH_4^+ salt, transforms to the latter upon dissolution in dimethylformamide and addition of R_4N^+ cations.

The possibility of internal electron-transfer processes, mediated by the S_x^{2-} ligands, often presents the choice of more than one electronic ground-state description for a given complex. In such situations, encountered with complexes such as $[Mo_3O_2S_8]^{2-}$,[13] $[Mo_2S_9]^{2-}$,[1] or $[Mo_2OS_8]^{2-}$,[6] self-consistent spectroscopic and structural characteristics are used to arrive at realistic descriptions of electronic structure.

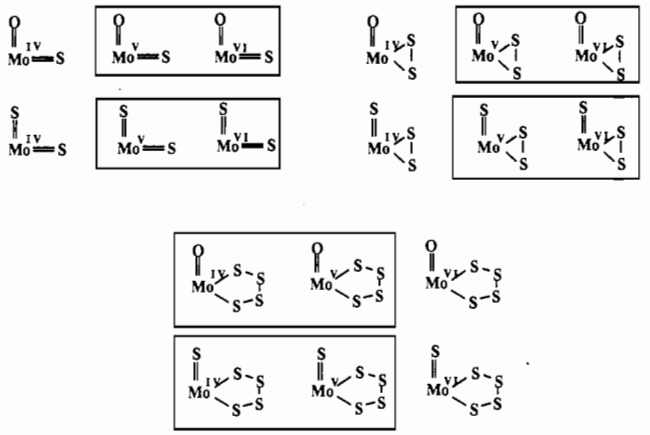

Figure 2. Functional groups in binary and tertiary thiomolybdate complexes with the Mo atom in oxidation states 4, 5, and 6. The known groups are enclosed within small frames.

A number of specific "functional groups", often characterized by distinct reactivity properties, can be identified in molybdothioanions that contain Mo in various formal oxidation states. Assignments of the formal oxidation levels of the Mo ions in these groups (Figure 2) are based on the crystallographically or spectroscopically determined number and types of S_x^{2-} ligands present in the "parent" complexes. An examination of Figure 1 shows certain trends in ligand preferences associated with the formal oxidation state of the Mo atoms. Thus, the S_4^{2-} ligand is found coordinated only to the larger Mo^{IV} and Mo^V ions. Similarly, more than one terminal E^{2-} ligands (E = S, O) are found mainly with groups that formally contain Mo^{VI}.

A systematic study of the reactivity characteristics of these functional groups (Figure 2) is expected to provide basic insight relevant to the chemistry that prevails in the catalytic hydrodesulfurization reaction (HDS). This reaction is carried out under H_2 at high temperatures and pressures and is used for the removal of sulfur (as H_2S) from organosulfur compounds present in crude petroleum.[20] The catalyst consists of "sulfided" molybdates supported on γ-Al_2O_3 and usually contains Co^{II} or Ni^{II} as promoter ions. It has been suggested[21] that HDS catalysis occurs at the edges rather than the basal planes of the γ-Al_2O_3-supported MoS_2 crystallites,[21] and the promotion effects of Co^{II} or Ni^{II} may occur at the same sites.

Any of the groups shown in Figure 2 may be present on the edges of the catalytically important MoS_2 particles. Cognizant of this fact our research efforts in recent years have been directed toward an understanding of the comparative reactivities of such groups in soluble molybdenum sulfide complexes. In this paper we report on the reactivity characteristics of several of these functional groups, with the electrophilic alkyne dicarbomethoxyacetylene (DMA). The latter has been used previously in reactions probing the reactivity of coordinated S_x^{2-} ligands.[21,22] The synthesis, possible reaction pathways, and detailed structural characterization of the complexes $[Et_4N]_2[MoO(S_2C_2(CO_2Me)_2)_2]$ (I), *anti*-$[Et_4N]_2[Mo_2O_2S_2(S_2C_2(CO_2Me)_2)_2]$ (II), *syn*-$[Ph_4P]_2[Mo_2O_2S_2(S_2C_2(CO_2Me)_2)_2]\cdot 2DMF$ (III), $[Ph_4P]_2$-

(2) (a) Miller, K. F.; Bruce, A. E.; Corbin, J. L.; Wherland, S.; Stiefel, E. I. *J. Am. Chem. Soc.* **1980**, *102*, 5102. (b) Pan, W. H.; Harmer, M. A.; Halbert, T. R.; Stiefel, E. I. *J. Am. Chem. Soc.* **1984**, *106*, 459.
(3) (a) Draganjac, M.; Simhon, E.; Chan, L. T.; Kanatzidis, M.; Baenziger, N. C.; Coucouvanis, D. *Inorg. Chem.* **1982**, *21*, 3321. (b) Clegg, W.; Christou, G.; Garner, C. D.; Sheldrick, G. M. *Inorg. Chem.* **1981**, *20*, 1562.
(4) Cohen, S. A.; Stiefel, E. I. *Inorg. Chem.* **1985**, *24*, 4657.
(5) Pan, W. H.; Leonowicz, M. E.; Stiefel, E. I. *Inorg. Chem.* **1983**, *22*, 672.
(6) Coucouvanis, D.; Sang-Man Koo, *Inorg. Chem.* **1987**, *26*, 2400.
(7) Muller, A.; Romer, M.; Romer, C.; Reinsch-Vogel, U.; Bogge, H.; Schimanski, U. *Monatsh. Chem.* **1985**, *116*, 711.
(8) Muller, A.; Hellmann, W.; Romer, C.; Romer, M.; Bogge, H.; Jostes, R.; Schimanski, U. *Inorg. Chim. Acta* **1984**, *83*, L75–L77 ($[(MoS_4)_2Mo(O)]^{2-}$).
(9) Clegg, W.; Mohan, N.; Muller, A.; Neumann, A.; Rittner, W.; Sheldrick, G. M. *Inorg. Chem.* **1980**, *19*, 2066.
(10) Toupadakis, A.; Coucouvanis, D. Manuscript in preparation.
(11) Hadjikyriacou, A. I. Ph.D. Thesis, University of Michigan, 1988.
(12) Muller, A.; Diemann, E.; Jostes, R.; Bogge, H. *Angew. Chem., Int Ed. Engl.* **1981**, *20*, 934.
(13) (a) Do, Y.; Simhon, E. D.; Holm, R. H. *Inorg. Chem.* **1985**, *24*, 2827. (b) Coucouvanis, D.; Toupadakis, A.; Hadjikyriacou, A. I. *Inorg. Chem.* **1988**, *27*, 3272. (c) Xin, X.; Jin, G.; Wang, B.; Pope, M. T. *Inorg. Chem.* **1990**, *29*, 553. (d) Coucouvanis, D.; Toupadakis, A.; Koo, Sang-Man. Manuscript in preparation.
(14) (a) Coucouvanis, D.; Hadjikyriacou, A. *Inorg. Chem.* **1987**, *26*, 1. (b) Xintao, W.; Shaofeng, L.; Lianyong, Z.; Quangjin, W.; Jiaxi, L. *Inorg. Chim. Acta* **1987**, *133*, 43. (c) Hadjikyriacou, A. I.; Coucouvanis, D. *Inorg. Chem.* **1989**, *28*, 2169. (d) Mennemann, K.; Mattes, R. *Angew. Chem., Int. Ed. Engl.* **1977**, *16*, 260. (e) Chandrasekaran, J.; Ansari, M. A.; Sarkar, S. *Inorg. Chem.* **1988**, *27*, 3663.
(15) Berzelius, J. J. *Poggendorffs Ann. Phys. Chem.* **1826**, *7*, 262; **1826**, *8*, 269.
(16) Muller, A.; Bhattacharyya, R. G.; Pfeferkorn, B. *Chem. Ber.* **1979**, *112*, 778.
(17) For the neutral free atoms, a compilation of Roothaan–Hartree–Fock atomic wave functions[18] shows the sulfur 3p orbitals with an energy of −0.43694 au and the molybdenum 4d(s^1d^5) with an energy of −0.34811 au. The localization of partial positive charge on the Mo and partial negative charge on the S is expected to bring these energies even closer together.
(18) Clementi, E.; Roetti, C. *At. Data Nucl. Data Tables* **1974**, *14*, 3.
(19) Muller, A.; Nolte, W. O.; Krebs, B. *Inorg. Chem.* **1980**, *19*, 2835.
(20) (a) Massoth, F. E. *Adv. Catal.* **1978**, *27*, 265. (b) Topsoe, J.; Clausen, B. S. *Catal. Rev.—Sci. Eng.* **1984**, *26*, 395. (c) Weisser, O.; Landa, S. *Sulfide Catalysts: Their Properties and Applications*; Pergamon Press: London, 1973.
(21) Stiefel, E. I.; Halbert, T. R.; Coyle, C. L.; Wei, L.; Pan, W.-H.; Ho, T. C.; Chianelli, R. R.; Daage, M. *Polyhedron* **1989**, *8*, 1625–1629.
(22) (a) Giolando, D. M.; Rauchfuss, T. B.; Rheingold, A. L.; Wilson, S. R. *Organometallics* **1987**, *6*, 667–675. In this paper Table IV contains an extensive compilation of metal-promoted dithiolene syntheses. (b) Kanatzidis, M. G.; Coucouvanis, D. *Inorg. Chem.* **1984**, *23*, 403.

$[Mo(S_2C_2(CO_2Me)_2)_3]\cdot DMF\cdot C_6H_6$ (IV), and $[Ph_4P]_2[Mo_2S_2(S_2C_2(CO_2Me)_2)_4]\cdot 2CH_2Cl_2$ (V) are presented. Preliminary accounts of the structures of I,[23] IV,[24] and V[23] have been reported previously. The syntheses and structural characterization of W/Se complexes, exactly analogous to IV and V, were reported recently.[25]

Experimental Section

(1) Synthesis. The chemicals in this work were used as purchased. Acetonitrile (CH_3CN), dichloromethane (CH_2Cl_2), and diethyl ether were distilled over calcium hydride. Dimethyl acetylenedicarboxylate (DMA) was distilled under reduced pressure at about 50 °C. All syntheses using oxothiomolybdate complexes were carried out under air. Those with thiomolybdate complexes were carried out in an inert atmosphere by using a Vacuum Atmospheres Dri-Lab glovebox filled with prepurified nitrogen, unless otherwise specified.

Bis(tetraethylammonium) Bis(1,2-dicarbomethoxy-1,2-ethylenedithiolato)oxomolybdate(IV) ($[Et_4N]_2[MoO(S_2C_2(CO_2Me)_2)_2]$ (I)). An amount of $(Et_4N)_2[MoO(S_4)_2]$[3] (2.0 g, 3.18 mmol), recrystallized from a DMF/2-propanol mixture, was dissolved under air in 500 mL of CH_3CN to give a yellow-orange solution. To this solution was added 0.90 mL (7.32 mmol) of dimethyl acetylenedicarboxylate (DMA). The reaction mixture was stirred for 30 min and then concentrated to 20–30 mL in vacuo. The concentrated solution was filtered, and to the filtrate was added 100 mL of THF. After standing for 10 h, the supernatant solution was decanted, and the solid left in the container was washed with three 30-mL portions of THF. The crude product so obtained was redissolved in a minimum amount of CH_3CN to give a brown-red solution. To this concentrated solution was added 100 mL of THF. After the solution was left standing for 10 h, brown-red needles of the product formed and were isolated, washed with THF and diethyl ether, and dried. The yield after drying was 1.20 g or 48%. Anal. Calcd for $C_{28}H_{52}N_2MoS_4O_9$ (MW 784): C, 42.85; H, 6.68; Mo, 12.22; S, 16.34; N, 3.57. Found: C, 42.91; H, 6.85; Mo, 12.38; S, 16.30; N, 3.63. ^1H NMR in DMSO-d_6: δ 3.62 (s, 12 H), 3.08 (q, 16 H), 1.08 (t, 24 H). FT-IR (CsI pellet, cm^{-1}): ν(C=O), 1727 (vs), 1714 (vs), 1704 (vs); ν(Mo=O), 914 (s); ν(Mo—S), 388 (w), 348 (w). UV/vis (DMF solution, 10^{-3} M, nm): 360, 460 (sh), 550.

Bis(tetraethylammonium) Bis(1,2-dicarbomethoxy-1,2-ethylenedithiolato)*anti*-bis((μ-sulfido)oxomolybdate(V)) ($[Et_4N]_2[anti\text{-}\{Mo_2(O)_2(\eta\text{-}S)_2\}(\eta^1\text{-}S\text{-}\eta^1\text{-}SC_2(CO_2Me)_2)_2]$ (II)). To a stirred solution of $(Et_4N)_2(Mo_2O_2S_9)$[14c] (1 g, 1.3 mmol) in 30 mL of CH_3CN was added 0.32 mL (2.6 mmol) of DMA. After being stirred for 15 min, the solution was cooled to 4 °C over a period of 12 h. The solid that formed was filtered out and washed with acetone. The crude product so obtained (0.23 g, 20% yield) was dissolved in 30 mL of DMF and afforded 0.20 g of a yellow microcrystalline solid after the addition of 60 mL of diethyl ether and standing at 4 °C for 12 h. Anal. Calcd for $C_{28}H_{52}N_2Mo_2S_6O_{10}$ (MW 960): C, 34.96; H, 5.41; N, 2.91; Mo, 19.96; S, 19.98. Found: C, 35.29; H, 5.77; N, 2.75; Mo, 19.53; S, 20.54. ^1H NMR in DMSO-d_6 vs TMS: δ 3.703 (s, 12 H), 3.154 (q, 16 H), 1.124 (t, 24 H). In CD_3CN solution the CH_3O_2C singlet appears at 3.759 ppm. FT-IR (KBr pellet, cm^{-1}): ν(C=O), 1727 (s), 1693 (s); ν(C—O—C), 1245 (s); ν(Mo=O), 923 (s), 911 (m); ν(Mo-S_b), 462 (w). UV/vis (DMF solution, 10^{-3} M, nm): 318, 380 (sh).

Bis(tetraethylammonium) Bis(1,2-dicarbomethoxy-1,2-ethylenedithiolato)*syn*-bis((μ-sulfido)oxomolybdate(V)) ($[Et_4N]_2[syn\text{-}\{Mo_2(O)_2(\mu\text{-}S)_2\}(\eta^1\text{-}S\text{-}\eta^1\text{-}SC_2(CO_2Me)_2)_2]$). **Method A.** An amount of $(Et_4N)_2[Mo_2O_2S_8]$[11] (2.00 g, 2.70 mmol) was dissolved in 110 mL of CH_3CN. To the red-orange solution was added 0.66 mL (5.41 mmol) of DMA with stirring. Within a few minutes the color of the solution turns dark brown with a yellow-green cast. After 50–60 min elemental sulfur is evident in suspension. The mixture was allowed to stand for 24 h and was filtered, and the filtrate was brought to near dryness under vacuum. The brown oil that remained was washed with three 30-mL portions of diethyl ether and two 30-mL portions of CS_2. Additional washings with ether and a final washing with 15 mL of acetone left as a residue a yellow powder. This yellow powder was extracted into 100 mL of acetone, and 100 mL of diethyl ether was added. When the solution was left standing, a yellow microcrystalline solid formed and was isolated and dried (0.9 g, 35% yield). Anal. Calcd for $C_{28}H_{52}N_2Mo_2S_6O_{10}$ (MW 960): C, 34.96; H, 5.41; N, 2.91; Mo, 19.96; S, 19.98. Found: C, 34.50; H, 5.30; N, 2.80; Mo, 19.75; S, 19.50. FAB$^+$ (in "magic bullet"[26]): *m/e* 1090 (P + Et_4N^+), 960 (P). FAB$^-$ (in "magic bullet"[26]): *m/e* 830 (P − Et_4N^+). Data are as follows for the ligand protons. ^1H NMR: in CD_3CN vs TMS, δ 3.774 (s, 12 H); in DMSO-d_6 vs TMS, δ 3.717 (s, 12 H); in DMF-d_7 vs TMS, δ 3.767 (s, 12 H). FT-IR (KBr pellet, cm^{-1}): ν(C=O), 1727 (s), 1693 (s); ν(C—O—C), 1245 (s); ν(Mo=O), 923 (s), 911 (m); ν(Mo—S_b), 462 (w). UV/vis (DMF solution, 10^{-3} M, nm): 318, 380 (sh).

Method B. Acid-Catalyzed Isomerization of the Anti Isomer (II). To a suspension of 0.1 g of $[Et_4N]_2[anti\text{-}\{Mo_2(O)_2(\mu\text{-}S)_2\}(\eta^1\text{-}S\text{-}\eta^1\text{-}SC_2(CO_2Me)_2)_2]$ (II) in 10 mL of acetone was added five drops of concentrated aqueous HCl. The suspension was stirred for ~7 h and then refluxed for 20 min. To the clear solution, after it was cooled to ambient temperature, was added a large excess of ether. The solid product was isolated and was recrystallized from an acetone–ether mixture to give yellow thin needles in nearly quantitative yield. The ^1H NMR spectrum of this compound was found identical with the one obtained by method A above.

Bis(tetraphenylphosphonium) Bis(1,2-dicarbomethoxy-1,2-ethylenedithiolato)*syn*-bis((μ-sulfido)oxomolybdate(V)) ($[Ph_4P]_2[syn\text{-}\{Mo_2(O)_2(\mu\text{-}S)_2\}(\eta^1\text{-}S\text{-}\eta^1\text{-}SC_2(CO_2Me)_2)_2]\cdot 2DMF$ (III)). To a solution of $(Ph_4P)_2(Mo_2OS_7)\cdot DMF$[6] (0.5 g, 0.42 mmol) in 50 mL of DMF was added a catalytic amount of elemental sulfur (~0.02 g). After the mixture was stirred for ca. 2 min, 0.2 mL of DMA (excess) was added and the solution was stirred for 2 h at 90 °C. After the mixture was cooled to ambient temperature, diethyl ether was added (150 mL). When the solution was allowed to stand for 2 days, a greenish yellow crystalline product formed and was isolated. The product was washed with 30-mL portions of diethyl ether, ethanol, and diethyl ether. The yield after drying in vacuum was 0.38 g (62%). FT-IR (KBr disk, cm^{-1}): ν(C=O), 1720 (s), 1694 (s); ν(C—O—C), 1239 (s); ν(Mo=O), 942 (m). Anal. Calcd for $C_{66}H_{66}P_2Mo_2S_6O_{12}$ (MW, 1524): C, 52.00; H, 4.30; Mo, 12.65; S, 12.65. Found: C, 52.3; H, 4.25; Mo, 12.30; S, 12.10.

Bis(tetraphenylphosphonium) Tris(1,2-dicarbomethoxy-1,2-ethylenedithiolato)molybdate(IV)–Dimethylformamide–Benzene ($[Ph_4P]_2[Mo(S_2C_2(CO_2Me)_2)_3]\cdot DMF\cdot C_6H_6$ (IV)). Method A. An amount of $(Ph_4P)_2MoS_4$[27] (0.5 g, 0.28 mmol) was dissolved in 50 mL of DMF, and to the solution was added with stirring 2.0 g (7.2 mmol) of solid $C_7H_7SSSC_7H_7$.[28] To the clear solution was added 2 mL (16 mmol) of DMA, and the resulting mixture was heated to 80 °C for 10 min. After the solution was cooled to ambient temperature, 150 mL of benzne were added and the solution was allowed to stand for 12 h. The resulting dark green crystals (0.2 g, 25% yield) were isolated and washed with three 30-mL portions of diethyl ether before drying. Anal. Calcd for $C_{75}H_{71}P_2MoS_6NO_{13}$ (MW 1544.7): C, 53.60; H, 4.60; Mo, 6.21; S, 12.43. Found: C, 54.44; H, 4.16; Mo, 6.36; S, 13.54. X-ray powder pattern spacings (Å): 12.4 (s), 11.0 (s), 9.4 (vw), 8.4 (s), 8.0 (m), 4.55 (m), 4.40 (m), 4.30 (m), 4.10 (m), 3.83 (w), 3.68 (w), 3.53 (w), 3.30 (w), 3.20 (w), 3.07 (w), 2.95 (w), 2.75 (w). The X-ray powder pattern of the bulk of this compound was found identical with that calculated from single-crystal data.

Method B. The same compound can be obtained in 15% yield from the reaction of $(Ph_4P)_2MoS(S_4)_2$ with a 60-fold excess of DMA in boiling CH_3CN.

Bis(tetraphenylphosphonium) Tris(1,2-dicarbomethoxy-1,2-ethylenedithiolato)tungstate(IV)–Dimethylformamide–Benzene ($[Ph_4P]_2[W(S_2C_2(CO_2Me)_2)_3]\cdot DMF\cdot C_6H_6$). Red-violet crystals of this complex were obtained from $(Ph_4P)_2WS_4$ in 43% yield in a synthetic procedure exactly analogous to the one described for the synthesis of the Mo complex (method A). Anal. Calcd for $C_{75}H_{71}P_2WS_6NO_{13}$: C, 55.18; H, 4.35; W, 11.28; S, 11.77; P, 3.80. Found: C, 54.27; H, 3.88; W, 11.65; S, 12.35; P, 3.89. This compound was found X-ray isomorphous to the analogous Mo derivative.

Bis(tetraphenylphosphonium) Bis(μ-thio)bis[bis(1,2-dicarbomethoxy-1,2-ethylenedithiolato)molybdate(V)]–2-Methylene Chloride ($[Ph_4P]_2[Mo_2S_2(S_2C_2(CO_2Me)_2)_4]\cdot 2CH_2Cl_2$ (V)). Method A. An amount of $(Ph_4P)_2[Mo_2S_{10}/S_{12}]$[3] (0.52 g, 0.42 mmol) was dissolved in 300 mL of CH_3CN. To this solution was added slowly, with stirring, 0.21 mL (1.67 mmol) of freshly distilled DMA. The reaction mixture was refluxed for 30 min and underwent color changes from brown to purple to finally green. After cooling to ambient temperature, the solvent was removed under vacuum and the dry residue was washed with 30 mL of CH_2Cl_2. The residue was isolated by filtration and was dissolved in the minimum required amount of a 6:1 DMF/CH_2Cl_2 mixture to give a green solution. Slow diffusion of diethyl ether to this solution afforded 0.22 g of green crystals of the product (26% yield). Anal. Calcd for $C_{74}H_{68}P_2Mo_2S_{10}$-

(23) Coucouvanis, D.; Hadjikyriacou, A. I.; Draganjac, M.; Kanatzidis, M. G.; Ileperuma, O. *Polyhedron* **1986**, *5*, 349.
(24) Draganjac, M.; Coucouvanis, D. *J. Am. Chem. Soc.* **1983**, *105*, 139.
(25) Ansari, M. A.; Mahler, C. H.; Ibers, J. A. *Inorg. Chem.* **1989**, *28*, 2669–2674.
(26) This matrix is a 3:1 mixture of dithiothreitol and dithioerythritol.
(27) Hadjikyriacou, A. I.; Coucouvanis, D. *Inorg. Synth.* **1990**, *27*, 39–47.
(28) Coucouvanis, D.; Kanatzidis, M. G.; Simhon, E.; Baenziger, N. C. *J. Am. Chem. Soc.* **1982**, *104*, 1874.

Table I. Summary of Crystal Data and Intensity Collection and Structure Refinement Data for $(Et_4N)_2MoO[S_2C_2(CO_2Me)_2]_2$ (I), *anti*-$(Et_4N)_2Mo_2O_2S_2[S_2C_2(CO_2Me)_2]_2$ (II), *syn*-$(Ph_4P)_2Mo_2O_2S_2[S_2C_2(CO_2Me)_2]_2 \cdot 2DMF$ (III), $(Ph_4P)_2Mo[S_2C_2(CO_2Me)_2]_3 \cdot DMF \cdot C_6H_6$ (IV), and $(Ph_4P)_2Mo_2S_2[S_2C_2(CO_2Me)_2]_4 \cdot 2CH_2Cl_2$ (V)

compd	I	II	III	IV	V
chem formula	$C_{28}H_{52}N_2O_9S_4Mo$	$C_{28}H_{52}N_2O_{10}S_6Mo_2$	$C_{66}H_{66}N_2O_{12}P_2S_6Mo_2$	$C_{75}H_{71}NO_{13}P_2S_6Mo$	$C_{74}H_{68}O_{16}P_2Cl_4S_{10}Mo_2$
MW	784	960	1524.18	1544.71	1928
a, Å	17.664 (4)	9.004 (2)	12.919 (4)	22.907 (14)	12.778 (2)
b, Å	9.979 (2)	8.975 (3)	14.863 (6)	14.619 (9)	13.616 (3)
c, Å	21.363 (4)	13.904 (2)	18.844 (6)	43.746 (21)	13.898 (3)
α, deg	90.0	90.53 (2)	95.86 (3)	90.00	105.62 (2)
β, deg	100.5 (2)	102.04 (1)	102.61 (2)	95.34 (5)	98.80 (1)
γ, deg	90.0	112.11 (2)	93.74 (3)	90.00	110.10 (1)
V, Å^3; Z	3702 (1); 4	1013 (1); 1	3498 (1); 2	14586; 8	2104.8 (7); 1
d_{calcd}, g/cm^3	1.41	1.57	1.45	1.27	1.52
d_{obsd}, g/cm^3 [a]	1.40	1.56	1.448	1.35	1.50
space group	$P2_1/c$	$P\bar{1}$	$P\bar{1}$	$C2/c$	$P\bar{1}$
cryst dimens, mm	0.47 × 0.18 × 0.25	0.11 × 0.15 × 0.22	0.17 × 0.47 × 0.15	0.1 × 0.04 × 0.32	
abs coeff μ, cm^{-1}	6.2	9.16	6.04	4.4	
radiation	Mo Kα	Mo Kα	Mo Kα	Mo Kα	Mo Kα
no. of data collcd[b]	3892	2079	$2\theta_{max} = 45$	$6 < 2\theta < 40$[c]	$2\theta_{max} = 40$
min–max scan speed	3.0–29.3	2.9–29.3	2.5–12		
no. of unique data	2997	1841	9118	7155	
no. of data used in refinement ($F_o^2 > 3s(F_o^2)$)	2704	1774	6350	2637	2412
no. of atoms in asym unit	106	50	145	168	88
no. of variables	393	217	775	389	313
R, %[c,d]	4.94	2.12	4.63	6.9	6.26
R_w, %[c,d]	5.03	2.43	4.41	7.70	6.60

[a] By flotation in CCl_4/hexane mixture. [b] At ambient temperature. [c] ω-scan technique. [d] $R_1 = (\sum||F_o| - |F_c||)/\sum|F_o|$. $R_2 = [\sum_w((|F_o| - |F_c|)^2/\sum_w|F_o|^2]^{1/2}$.

Cl_4O_{16} (MW 1928): C, 47.06; H, 3.55; Mo, 9.94; S, 16.61. Found: C, 47.54; H, 3.69; Mo, 9.52; S, 16.38. FT-IR (KBr pellet, cm^{-1}): ν(C=O), 1705 (s), 1675 (s), 1650 (m); ν(C—O—C), 1220 (vs). UV/vis (DMF solution, 10^{-3} M, nm): 380, 430 (sh), 582, 680.

Method B. An amount of $(Ph_4P)_2[Mo_2S_4(CS_4)_2 \cdot {}^1/_2DMF]$[29] (0.26 g, 0.21 mmol) was dissolved with stirring in 50 mL of CH_3CN, and to this solution was added 0.10 mL of freshly distilled DMA. The reaction mixture was refluxed for 30 min. The dark green solution was cooled to ambient temperature, and the solvent was removed under vacuum. A procedure identical with the one described in method A above was followed, and 0.10 g of green crystals were isolated (26% yield). These crystals were found to be identical with those obtained by method A.

Thermal Isomerization of the Et_4N^+ Salt of [|*syn*-$Mo_2(O)_2(\mu$-$S)_2$|-*cis*-(η^1-S-η^1-CSC$(CO_2Me)_2)_2]^{2-}$ into the Corresponding [{*syn*-$Mo_2(O)_2(\mu$-$S)_2$}(η^1-S-η^1-$SC_2(CO_2Me)_2)_2]^{2-}$ Dithiolene Complex. An amount of the *cis*-bis(vinyl disulfide) complex (1.0 g, 1.04 mmol), obtained according to the synthetic procedure previously described in the literature,[30] was suspended in 50 mL of DMF. The mixture was heated with stirring to 80–90 °C for 1 h. After the solution was cooled to ambient temperature and upon addition of a large excess of diethyl ether, a solid formed and was isolated. The crude product was extracted in acetone and crystallized upon addition of diethyl ether. ^{1}H NMR in DMSO-d_6 vs TMS: δ 3.71 (s, 12 H), 3.10 (q, 16 H), 1.15 (t, 24 H).

Bis(tetraethylammonium) (1,2-Dicarbomethoxy-2-vinyl disulfido)-(tetrasulfido)*syn*-bis($(\mu$-sulfido)oxomolybdate(V)) ($[Et_4N]_2[(\eta^1$-S-η^1-CSC$(COOMe)_2)(S_4)$-*syn*-$\{Mo_2(O)_2(\mu$-$S)_2\}]$ (VI)). An amount of $(Et_4N)_2Mo_2O_2S_8$ (1.00 g, 1.35 mmol) was dissolved in 60 mL of CH_3CN under air. To the orange-red solution was added 0.34 mL (1.35 mmol) of DMA, and the reaction mixture was stirred at ambient temperature for 10 min. To the yellow-brown solution that resulted was added 300 mL of ether, and the mixture was stored at −20 °C. After 8 h, the supernatant solution was decanted and the solid residue in the container was washed with three portions of diethyl ether. The solid was further suspended in 10 mL of acetone, and the mixture was stirred for 2 min and filtered. The yellow powder so obtained was washed thoroughly with diethyl ether and dried. The yield after drying was 0.9 g. Anal. Calcd for $C_{22}H_{46}Mo_2O_6S_8N_2$ (MW 894): C, 29.93; H, 5.22; Mo, 21.77; S, 29.02. Found: C, 29.11; H, 5.21; Mo, 23.03; S, 29.21. FT-IR (CsI pellet, cm^{-1}): ν(C=O), 1719 (s), 1693 (s), 1704 (vs); ν(Mo=O), 945 (vs); ν(Mo—S), 462 (w), 375 (vw), 354 (vw), 337 (w), 327 (w).

(2) Physical Methods. Visible and ultraviolet spectra were obtained on a Cary Model 219 spectrophotometer. Infrared spectra were recorded on a Nicolet 60 SX FT-IR spectrometer at a resolution of 4 cm^{-1} in CsI or KBr disks. Proton NMR spectra were obtained on a Bruker 300-MHz pulse FT NMR spectrometer with Me_4Si as internal standard. Chemical shifts are reported in parts per million (ppm). Electrochemical measurements were performed either with a PAR Model 173 potentiostat/galvanostat and a PAR Model 175 universal programmer or with BAS 100A electrochemical analyzer. The electrochemical cells used had platinum working and auxiliary electrodes. As a reference electrode, either a saturated calomel electrode or a Ag/AgCl electrode was used. All solvents used in the electrochemical measurements were properly dried and distilled, and tetra-*n*-butylammonium perchlorate (Bu_4NClO_4) was used as the supporting electrolyte. Normal concentrations used were 0.001–0.005 M in electroanalyte and 0.1 M in supporting electrolyte. Unless otherwise stated the scan speeds were 100 mV/s. Purified argon was used to purge the solutions prior to the electrochemical measurements.

X-ray Diffraction Measurements. (a) Collection of Data. Single crystals of $[Et_4N]_2[MoO(S_2C_2(CO_2Me)_2)_2]$ (I) and *syn*-$[Ph_4P]_2$-$[Mo_2O_2S_2(S_2C_2(CO_2Me)_2)_2] \cdot 2DMF$ (III) were obtained by the slow diffusion of diethyl ether into DMF solutions of the complexes. Crystals of *anti*-$[Et_4N]_2[Mo_2O_2S_2(S_2C_2(CO_2Me)_2)_2]$ (II) were obtained from a saturated CH_3CN solution by slow evaporation of the solvent under air. Single crystals of $[Ph_4P]_2[Mo(S_2C_2(CO_2Me)_2)_3] \cdot DMF \cdot C_6H_6$ (IV) were obtained by the slow diffusion of benzene into a DMF solution of the complex. Single crystals of $[Ph_4P]_2[Mo_2S_2(S_2C_2(CO_2Me)_2)_4] \cdot 2CH_2Cl_2$ (V) were obtained by the slow diffusion of diethyl ether into a 6:1 DMF/CH_2Cl_2 solution of the complex.

A single crystal for each complex was carefully chosen and mounted in a thin-walled, sealed capillary tube. Diffraction data for I–III and V were collected on a Nicolet P3/F four-circle, computer-controlled diffractometer at ambient temperature. Intensity data for IV were obtained on a Picker-Nuclear four-circle diffractometer equipped with scintillation counter and pulse-height analyzer and automated by a DEC PDP8-I computer and disk with FACS-I DOS software. Graphite-monochromatized Mo Kα radiation ($2\theta_m = 12.50°$) was used for data collection and cell dimension measurements (λ(Kα) = 0.7107 Å).

Intensity data for all crystals were obtained by using graphite-monochromatized Mo Kα radiation with a θ–2θ step-scan technique. Throughout the data collection three standard reflections were monitored every 100 reflections to monitor crystal and instrumental stability. No crystal decay was observed. Accurate cell parameters were obtained from a least-squares fit of the angular settings (2θ, ω, ϕ, χ) of 25 machine-centered reflections with 2θ values between 20 and 30°. Details concerning crystal characteristics and X-ray diffraction methodology are shown in Table I.

(b) Reduction of Data. The raw data were reduced to net intensities, estimated standard deviations were calculated on the basis of counting

(29) Coucouvanis, D.; Draganjac, M. *J. Am. Chem. Soc.* **1982**, *104*, 6820.
(30) Halbert, T. R.; Pan, W. H.; Stiefel, E. I. *J. Am. Chem. Soc.* **1983**, *105*, 5476.

statistics, Lorentz–polarization corrections were applied, and equivalent reflections were averaged. The estimated standard deviation of the structure factor was taken as the larger of that derived from counting statistics and that derived from the scatter of multiple measurements.

The least-squares program used minimizes $\Sigma w(|\Delta F|)^2$. The weighting function used throughout the refinement of the structure gives zero weight to those reflections with $F^2 < 3\sigma(F^2)$ and $w = 1/\sigma^2(F)$ to all others,[31] where $\sigma^2(F) = \sigma_1^2(F) + |(g)F^2|$ ($g = 0.0002$). No corrections for secondary extinction were applied to data sets I–V. The atomic scattering factors of the neutral atoms were used, and all the scattering factors[32] except those for hydrogen were corrected by adding real and imaginary terms to account for the effects of anomalous dispersion.[33] The spherical hydrogen scattering factor tables of Stewart et al.[34] were used.

Due to the small μ values (Table I) and the small size of the crystals, no absorption corrections were applied to the data.

(c) Determination of Structures. Three-dimensional Patterson synthesis maps along with the direct methods routine SOLV of the SHELXTL 84 package of crystallographic programs or MULTAN[35] (for IV) was employed to locate Mo or S atoms. Subsequent difference Fourier maps were used to locate all other non-hydrogen atoms in the asymmetric units.

$[Et_4N]_2[MoO(S_2C_2(CO_2Me)_2)_2]$ (I). After all non-hydrogen atoms were located it became apparent that one of the Et_4N^+ cations (N1, on a general position) was disordered. The disorder is such that two of the four ethyl chains occupy two positions each at half-occupancy. The CH_2 carbon atoms of the other two ethyl chains also occupy two positions each at half-occupancy. The CH_3 terminal carbon atoms in these chains are shared by each of the two half ethyl groups at full occupancy. An additional disorder problem was encountered with the $COOCH_3$ groups on one of the ligands. This ligand (S3S4C7C9...) shows the COOR groups in two orientations each at half-occupancy. The disorder is such that the OCH_3 groups, in two orientations for each of the COOR units, share a CH_3 carbon atom (C11 for the unit and C12 for the other) that occupies the site at full occupancy. Isotropic refinement of all non-hydrogen atoms with occupancy factors as indicated above gave an R value of 0.082. All non-hydrogen atoms except for three of the half-occupancy oxygen atoms (O6, O'6, O'9) in the disordered ligand and all atoms in the disordered Et_4N^+ cation (N1) were assigned anisotropic temperature factors, and the model was refined to a final R value of 0.050. The positions of the hyrogen atoms were calculated and included in the structure factor calculation but were not refined. This inclusion of the H atoms in the structure factor calculation did not improve the final R and R_w values that on convergence were 0.050 and 0.050, respectively. At this stage all parameter shifts were less than 20% of their estimated standard deviation.

***anti*-$[Et_4N]_2[Mo_2O_2S_2(S_2C_2(CO_2Me)_2)_2]$ (II).** The structure was solved by using the direct-methods routine SOLV of the SHELX84 crystallographic programs package. In the space group $P\bar{1}$ with $Z = 1$, the $[Mo_2O_2S_2(S_2C_2(CO_2Me)_2)_2]^{2-}$ dianion is required to reside on a crystallographic inversion center. The positions of the Mo and the bridging S atoms were initially located. The remaining non-hydrogen atoms in the anion and the cation were located in electron density maps following difference Fourier calculations. The tetraethylammonium cation in the asymmetric unit is located on a general position. All of the non-hydrogen atoms in the asymmetric unit were refined with isotropic temperature factors to convergence at $R = 0.062$. The refinement process then continued with full-matrix least-squares calculations after the assignment of anisotropic temperature factors to all non-hydrogen atoms. In these final refinement calculations the hydrogen atoms were included in the structure factor calculation (C–H = 0.95 Å) but were not refined. At convergence the final R and R_w values were 0.021 and 0.024, respectively. At this stage all parameter shifts were less than 10% of their estimated standard deviation.

***syn*-$[Ph_4P]_2[Mo_2O_2S_2(S_2C_2(CO_2Me)_2)_2]\cdot 2DMF$ (III).** The two Mo and all of the S atoms in the asymmetric unit were located by the direct-methods routine SOLV of the SHELX84 crystallographic programs package. The remaining non-hydrogen atoms were found in subsequent electron density maps following difference Fourier calculations. With the exception of the two DMF molecules of solvation all non-hydrogen atoms in the asymmetric unit were refined anisotropically. The DMF molecules were assigned isotropic temperature factors. One of the two DMF molecules was well behaved; the other was found disordered. Two orientations of the disordered DMF molecule are disposed in a manner that places the two $N(CH_3)_2$ at two $^1/_2$ occupancy positions and allows them to share the carbon and oxygen atom sites of the C=O functional group. As a result, the C=O carbon and oxygen sites are each occupied by $^1/_2$ C and $^1/_2$ O atoms. Both sites were assigned partial occupation by O atoms. The site occupation factor for these positions was determined as 0.875 (7 e^-). In the final refinement calculations the hydrogen atoms were included in the structure factor calculation (C–H = 0.95 Å) but were not refined. At convergence the final R and R_w values were 0.046 and 0.044, respectively, and all parameter shifts were less than 10% of their estimated standard deviation.

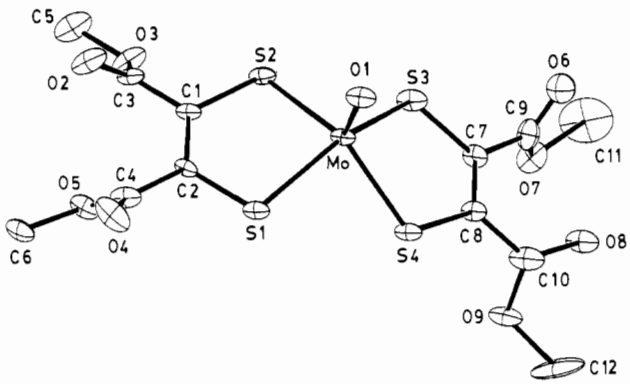

Figure 3. Structure and labeling of the $[MoO(S_2C_2(CO_2Me)_2)_2]^{2-}$ anion in I. Thermal motion is represented by 50% probability ellipsoids as drawn by ORTEP.[56]

$[Ph_4P]_2[Mo(S_2C_2(CO_2Me)_2)_3]\cdot DMF\cdot C_6H_6$ (IV). The refinement of all atoms with isotropic temperature factors in the monoclinic space group $C2/c$ gave a conventional R value of 0.076. Attempts to refine the anisotropic temperature factors on the atoms of the anion resulted in a small data to parameter ratio. Changing the criterion for rejection to $F^2 < 2\sigma(F^2)$ increased the number of usable data from 2637 to 3497. Refinement was continued along two pathways: One refinement was carried out with all atoms assigned isotropic temperature factors and the rejection criterion $F^2 < 3\sigma(F^2)$. The other refinement set the rejection criterion at $F^2 < 2\sigma(F^2)$, and the anion was refined with anisotropic temperature factors. This latter refinement converged to an R value of 0.086. Introduction of the hydrogen atoms at their calculated positions (0.95 Å from the carbon atoms) caused convergence to a final R value of 0.079 and an R_w of 0.078. The first refinement was then pursued with all atoms assigned isotropic temperature factors and the hydrogen atoms included at their calculated positions (0.95 Å from the carbon atoms). This refinement converged to an R value of 0.069 and an R_w of 0.077, and all parameter shifts were less than 15% of their estimated standard deviation.

$[Ph_4P]_2[Mo_2S_2(S_2C_2(CO_2Me)_2)_4]\cdot 2CH_2Cl_2$ (V). The heavy atoms in the centrosymmetric dimer were located by a combination of direct methods and Patterson techniques. All non-hydrogen atoms were located in subsequent difference Fourier maps. The atoms in the anion and the P atom of the cation were assigned anisotropic temperature factors with the exception of C6–C9 and C11 that showed small (rather insignificant) nonpositive-definite anisotropic temperature factor components and therefore were refined with isotropic temperature factors. The cation carbon atoms were refined isotropically. In the final cycles of refinement the hydrogen atoms were included at their calculated positions (0.95 Å from the carbon atoms) but were not refined. The refinement converged to an R value of 0.063 and an R_w of 0.066. The CH_2Cl_2 molecule in the asymmetric unit shows 3-fold positional disorder, as indicated by six $^1/_3$ occupancy sites for the Cl atoms around the common C atom. At this point all parameter shifts were less than 15% of their estimated standard deviation.

(d) Crystallographic Results. The final atomic positional parameters for $[Et_4N]_2[MoO(S_2C_2(CO_2Me)_2)_2]$ (I), *anti*-$[Et_4N]_2[Mo_2O_2S_2(S_2C_2(CO_2Me)_2)_2]$ (II), *syn*-$[Ph_4P]_2[Mo_2O_2S_2(S_2C_2(CO_2Me)_2)_2]\cdot 2DMF$ (III), $[Ph_4P]_2[Mo(S_2C_2(CO_2Me)_2)_3]\cdot DMF\cdot C_6H_6$ (IV), and $[Ph_4P]_2[Mo_2S_2(S_2C_2(CO_2Me)_2)_4]\cdot 2CH_2Cl_2$ (V) with standard deviations are shown in Tables II–VI. Intermolecular distances and angles are given in Table (VII). The numbering schemes for the anions in I–V are shown in Figures 3–7, respectively.

Synthesis

The formation of I, in the reaction of DMA with the $[(S_4)_2Mo{=}O]^{2-}$ anion under aerobic conditions, proceeds readily

(31) Grant, D. F.; Killean, R. C. G.; Lawrence, J. L. *Acta Crystallogr., Sect. B* **1969**, *B25*, 374.
(32) Doyle, P. A.; Turner, P. S. *Acta Crystallogr., Sect. A* **1968**, *A24*, 390.
(33) Cromer, D. T.; Liberman, D. J. *J. Chem. Phys.* **1970**, *53*, 1891.
(34) Stewart, R. F.; Davidson, E. R.; Simpson, W. T. *J. Chem. Phys.* **1965**, *42*, 3175.
(35) Main, P.; Woolfson, M. M.; Germain, G. *MULTAN: A Computer Program for the Automatic Solution of Crystal Structure*; University of York: York, England, 1971.

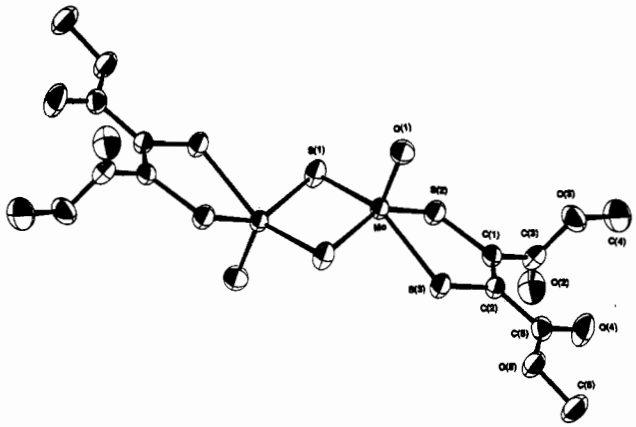

Figure 4. Structure and labeling of the *anti*-$[Mo_2O_2S_2(S_2C_2(CO_2Me)_2)_2]^{2-}$ anion in II. Thermal motion is represented by 50% probability ellipsoids as drawn by ORTEP.[56]

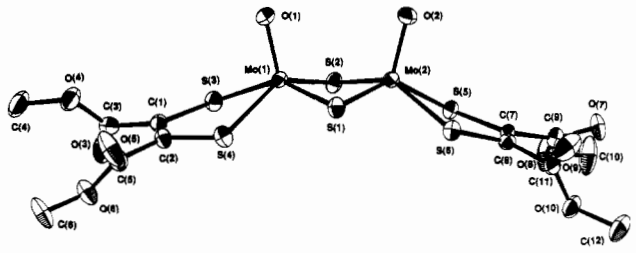

Figure 5. Structure and labeling of the *syn*-$[Mo_2O_2S_2(S_2C_2(CO_2Me)_2)_2]^{2-}$ anion in III. Thermal motion is represented by 50% probability ellipsoids as drawn by ORTEP.[56]

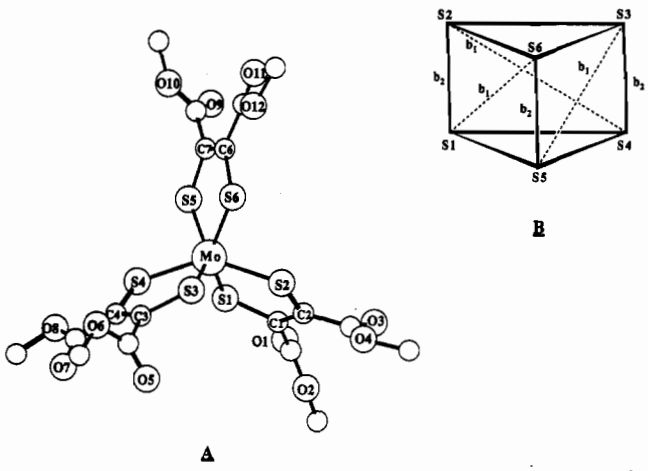

A

B

Figure 6. A: Structure and labeling of the $[Mo(S_2C_2(CO_2Me)_2)_3]^{2-}$ anion in IV. The carbon atoms of the carbomethoxy groups have not been labeled for clarity. B: Idealized trigonal prism and labeling after ref 42. (See text for details.)

at ambient temperature. This contrasts with the reaction of $[(S_4)_2Mo{=}O]^{2-}$ with CS_2 that does not give the analogous $[(CS_4)_2Mo{=}O]^{2-}$ complex. The latter is obtained only in the presence of Ph_3P that "activates" the coordinated S_4^{2-} ligands to electrophilic attack. This difference in reactivity between DMA and CS_2 may be attributed to the superior electrophilic character of the former with respect to the latter. The heterolytic cleavage of the relatively unreactive S_5^{2-} ligand in the $(RC_5H_4)_2Ti(S_5)$ complex has been reported to be affected by R_3P that facilitates further reaction with DMA with the eventual formation of the dithiolene ligand.[22a].

The dimeric Mo(V) oxothioanions $[(\eta^2\text{-}S_2)(O)Mo(\mu_2\text{-}S)_2Mo(O)(S_4)]^{2-}$ (VII) and $[(\eta^2\text{-}S_2)(O)Mo(\mu_2\text{-}S)_2Mo(O)(\eta^2\text{-}S_2)]^{2-}$ (VIII) show different overall reactivity with DMA under comparable reaction conditions (24 h, room temperature, CH_3CN).

Table II. Fractional Atomic Coordinates and Thermal Parameters for $[Et_4N]_2[MoO(S_2C_2(CO_2Me)_2)_2]$ (I)

atom	*x*	*y*	*z*	U^a
Mo1	0.2256 (0)	0.9148 (1)	0.2471 (0)	0.039
S1	0.2917 (1)	0.7834 (2)	0.1809 (1)	0.047
S2	0.1480 (1)	0.9774 (2)	0.1476 (1)	0.052
S3	0.2088 (1)	1.1412 (2)	0.2757 (1)	0.057
S4	0.3491 (1)	0.9434 (2)	0.3126 (1)	0.048
O1	0.1724 (3)	0.8146 (5)	0.2860 (2)	0.053
O2	0.0920 (5)	0.7698 (8)	0.0020 (3)	0.086
O3	0.1140 (4)	0.9887 (8)	0.0016 (3)	0.078
O4	0.2616 (5)	0.5713 (8)	0.0686 (3)	0.108
O5	0.2631 (4)	0.7405 (6)	0.0047 (3)	0.069
O6	0.2283 (10)	1.3276 (18)	0.3995 (8)	0.092
O7	0.3137 (11)	1.4164 (15)	0.3510 (7)	0.081
O8	0.4053 (10)	1.2298 (22)	0.4439 (10)	0.109
O9	0.4781 (7)	1.1433 (18)	0.3789 (7)	0.065
O′6	0.3411 (10)	1.3589 (22)	0.3880 (10)	0.121
O′7	0.2136 (18)	1.3819 (33)	0.3661 (13)	0.220
O′8	0.4139 (15)	1.1111 (29)	0.4588 (10)	0.144
O′9	0.4726 (11)	1.0814 (20)	0.4005 (10)	0.082
C1	0.1725 (5)	0.8673 (9)	0.0903 (4)	0.043
C2	0.2326 (5)	0.7851 (9)	0.1044 (4)	0.041
C3	0.1235 (5)	0.8685 (12)	0.0274 (5)	0.055
C4	0.2526 (5)	0.6896 (11)	0.0589 (5)	0.053
C5	0.0668 (8)	0.9979 (15)	−0.0609 (5)	0.111
C6	0.2760 (6)	0.6519 (11)	−0.0468 (5)	0.075
C7	0.2863 (6)	1.1790 (9)	0.3367 (4)	0.051
C8	0.3451 (6)	1.0974 (9)	0.3524 (4)	0.047
C9	0.2778 (8)	1.3117 (15)	0.3676 (6)	0.112
C10	0.4110 (7)	1.1335 (13)	0.4033 (6)	0.079
C11	0.2863 (12)	1.5366 (12)	0.3853 (8)	0.171
C12	0.5469 (7)	1.1496 (17)	0.4348 (8)	0.146
N2	0.0406 (4)	0.4985 (7)	0.1611 (3)	0.057
C21	0.0471 (6)	0.3608 (9)	0.1318 (5)	0.076
C22	0.0763 (7)	0.3612 (11)	0.0690 (5)	0.098
C23	0.1182 (5)	0.5675 (9)	0.1750 (4)	0.061
C24	0.1772 (7)	0.4977 (11)	0.2220 (7)	0.109
C25	0.0105 (5)	0.4745 (10)	0.2219 (4)	0.068
C26	0.0035 (6)	0.6006 (11)	0.2618 (5)	0.083
C27	−0.0123 (6)	0.5922 (10)	0.1170 (4)	0.074
C28	−0.0937 (6)	0.5381 (13)	0.0939 (5)	0.100
N1	0.4022 (4)	0.1991 (7)	0.1375 (4)	0.065
C13	0.4314 (9)	0.1318 (15)	0.2032 (7)	0.079
C14	0.5113 (11)	0.1802 (19)	0.2353 (9)	0.111
C15	0.4025 (9)	0.3547 (15)	0.1455 (7)	0.082
C16	0.3683 (11)	0.3924 (19)	0.2017 (9)	0.182
C17	0.3214 (9)	0.1447 (16)	0.1162 (7)	0.081
C18	0.2794 (9)	0.2109 (14)	0.0543 (7)	0.130
C19	0.4580 (11)	0.1781 (21)	0.0903 (9)	0.110
C20	0.4646 (17)	0.0313 (28)	0.0762 (12)	0.172
C13′	0.4863 (22)	0.2258 (37)	0.1211 (18)	0.079
C14′	0.5392 (23)	0.1396 (38)	0.2011 (19)	0.090
C15′	0.3813 (30)	0.2138 (52)	0.2015 (23)	0.133
C17′	0.3559 (26)	0.2780 (45)	0.0795 (21)	0.118
C19′	0.3673 (24)	0.0463 (42)	0.1195 (19)	0.105
C20′	0.4083 (28)	−0.0090 (46)	0.0666 (22)	0.113

[a] Equivalent isotropic temperature factor U_{eq} (Å^2) defined as one-third of the trace of the orthogonal U_{ij} tensor.

The former gives the bisdithiolene dimeric complex, $[\eta^1\text{-}S\text{-}\eta^1\text{-}SC_2(CO_2Me)_2)_2\text{-}syn\text{-}\{Mo_2(O)_2(\mu\text{-}S)_2\}]^{2-}$ (III) (eq 1), while the

$$[(\eta^2\text{-}S_2)(O)Mo(\mu_2\text{-}S)_2Mo(O)(\eta^2\text{-}S_4)]^{2-} + 2DMAD \rightarrow [(\eta^1\text{-}S\text{-}\eta^1\text{-}SC_2(CO_2Me)_2)_2\text{-}syn\text{-}\{Mo_2(O)_2(\mu_2\text{-}S)_2\}]^{2-} + \tfrac{3}{8}S_8 \quad (1)$$

$$[(\eta^2\text{-}S_2)(O)Mo(\mu_2\text{-}S)_2Mo(O)(\eta^2\text{-}S_2)]^{2-} + 2DMA \rightarrow [(\eta^1\text{-}S\text{-}\eta^1\text{-}CSC(CO_2Me)_2)_2\text{-}syn\text{-}\{Mo_2(O)_2(\mu_2\text{-}S)_2\}]^{2-} \quad (2)$$

latter gives the previously reported[30] and structurally characterized *cis-syn*-bis(vinyl disulfide) complex, $[cis\text{-}(\eta^1\text{-}S\text{-}\eta^1\text{-}CSC(CO_2Me)_2)_2\text{-}syn\text{-}\{Mo_2(O)_2(\mu_2\text{-}S)_2\}]^{2-}$ (IIIb) (eq 2). The reaction of VII with 1 equiv of DMA in CH_3CN at ambient temperature and with a short reaction time (~10 min) gives the "mixed-ligand" dimer $[(L)(O)Mo(\mu_2\text{-}S)_2Mo(O)(S_4)]^{2-}$ (L = $\eta^1\text{-}S\text{-}\eta^1\text{-}CSC(CO_2Me)_2$) (VI) (eq 3) and suggests that the reaction of DMA

$$[(\eta^2\text{-}S_2)(O)Mo(\mu_2\text{-}S)_2Mo(O)(S_4)]^{2-} + DMA \rightarrow [(\eta^1\text{-}S\text{-}\eta^1\text{-}CSC(CO_2Me)_2)(O)Mo(\mu_2\text{-}S)_2Mo(O)(S_4)]^{2-} \quad (3)$$

with the η^2-S_2^{2-} ligand is faster than that with the η^2-S_4^{2-} ligand. The reaction of VI with an additional 1 equiv of DMA at room temperature eventually leads to the bisdithiolene complex III (eq 4) that forms following isomerization of the vinyl disulfide ligands

$$[(\eta^1\text{-}S\text{-}\eta^1\text{-}CSC(CO_2Me)_2)(O)Mo(\mu_2\text{-}S)_2Mo(O)(S_4)]^{2-} + DMA \rightarrow [(\eta^1\text{-}S\text{-}\eta^1\text{-}SC_2(CO_2Me)_2)_2\text{-}syn\text{-}\{Mo_2(O)_2(\mu_2\text{-}S)_2\}]^{2-} + \tfrac{2}{8}S_8 \quad (4)$$

to dithiolenes. This isomerization, which occurs at ambient temperatures, undoubtedly is catalyzed by elemental sulfur that is present in solution as a result of S_2 dissociation from the η^2-S_4^{2-} ligand in VI. Indeed, in the absence of elemental sulfur the isomerization of IIIb to III is quite slow even at elevated temperatures (~70 °C). The catalytic effect of sulfur in such isomerizations has been demonstrated recently with the $[(Cp)(O)Mo^V(\mu\text{-}S)_2Mo^V(O)(L)]^-$ complex[36] (L = $[\eta^1\text{-}S\text{-}\eta^1\text{-}CSC(CO_2Me)_2]^{2-}$). The reaction of $(Mo_2O_2S_9)^{2-}$ with DMA affords a mixture of products with infrared spectra that suggest the presence of both the anti and syn isomers, II and III, respectively. The isolation of II was possible due to different solubility characteristics of the two isomers. A change of the Mo oxidation state, from +6 in $(Mo_2O_2S_9)^{2-}$ ligand to +5 in II or III suggests that internal electron transfer has taken place with oxidation of a S_x^{2-} ligand to elemental sulfur.

The reactions of either VII or $[(\eta^2\text{-}CS_4)(S)Mo(\mu_2\text{-}S)_2Mo(S)(\eta^2\text{-}CS_4)]^{2-}$ [29] with DMA (eqs 5 and 6) afford in low yield

$$[(\eta^2\text{-}S_4)(S)Mo(\mu_2\text{-}S)_2Mo(S)(\eta^2\text{-}S_2)]^{2-} + 4DMAD \rightarrow \{[(\eta^1\text{-}S\text{-}\eta^1\text{-}SC_2(CO_2Me)_2)_2Mo(S)(\mu_2\text{-}S)]_2\}^{2-} + \tfrac{2}{8}S_8 \quad (5)$$

$$[(\eta^2\text{-}CS_4)(S)Mo(\mu_2\text{-}S)_2Mo(S)(\eta^2\text{-}CS_4)]^{2-} + 4DMAD \rightarrow \{[(\eta^1\text{-}S\text{-}\eta^1\text{-}SC_2(CO_2Me)_2)_2Mo(S)(\mu_2\text{-}S)]_2\}^{2-} + 4CS_2 \quad (6)$$

(~25%) the dimer V. The same complex, V, also is obtained from the reaction of $[(S_4)_2Mo^{IV}(S)]^{2-}$ with DMA under aerobic conditions. Under anaerobic conditions the same reaction affords the trisdithiolene Mo^{IV} complex (IV).

Spectroscopic and Electrochemical Properties

A tabulation of selected infrared absorptions, electronic spectral data, and ^{1}H NMR spectral data of the complexes is presented in Table VIII. All of the complexes show two or three intense absorptions between 1650 and 1727 cm^{-1} (see Experimental Section). These absorptions are attributed to C=O vibrations of the two O=C—OCH_3 ligand groups that are often found in two orientations within the same dithiolene ligand (both in the plane and perpenticular to the plane of the MoC_2S_2 ring). An additional set of stretching vibrations associated with the ligand –O–C–OCH_3 chromophores are observed between 1200 and 1220 cm^{-1}. The Mo=O stretching frequencies of I–III and VI are characteristic and unexceptional. The ^{1}H NMR spectra of II and III are distinct and diagnostic for the syn and anti isomers. A thermal syn–anti isomerization is not evident at temperatures as high as 70 °C. The different orientations of the O=C—OCH_3 groups apparent in the solid-state structures (vide infra) for some of the complexes (I, II, IV, V) are not retained in solution, and free rotation around the C–C bonds of the dithiolene ligands results in equivalent CH_3 groups. The presence of only one set of CH_3 resonances in the spectrum of V also suggests that in solution the dithiolene ligands are fluxional and rapidly interchange the CH_3 groups cis and trans to the bridging sulfido ligands. The inequivalent CH_3 groups in the vinyl disulfide ligand in VI show δ values very similar to those observed in IIIb and support the structural assignment advanced for the former.

(36) Coucouvanis, D.; Toupadakis, A.; Koo, Sang-Man; Hadjikyriacou, A. *Polyhedron* **1989**, *8*, 1705–1716.

Table III. Fractional Atomic Coordinates and Thermal Parameters for *anti*-$[Et_4N]_2[Mo_2O_2S_2(S_2C_2(CO_2Me)_2)_2]$ (II)

atom	x	y	z	U^a
Mo	−0.0469 (0)	0.9084 (0)	0.5819 (0)	0.026
S1	0.0235 (1)	0.8284 (1)	0.4441 (1)	0.039
S2	−0.0848 (1)	0.7316 (1)	0.6540 (1)	0.034
S3	0.0490 (1)	1.0330 (1)	0.7497 (1)	0.033
O1	−0.2507 (3)	0.8001 (3)	0.5640 (2)	0.039
C1	0.1247 (4)	0.7718 (4)	0.7814 (3)	0.028
C2	0.1115 (4)	0.8992 (4)	0.8239 (2)	0.028
C3	0.1891 (6)	0.6577 (5)	0.8383 (3)	0.034
O2	0.3290 (4)	0.6730 (4)	0.8576 (2)	0.056
O3	0.0650 (3)	0.5332 (3)	0.8592 (2)	0.042
C4	0.1117 (6)	0.4136 (5)	0.9129 (3)	0.058
C5	0.1652 (4)	0.9381 (5)	0.9321 (3)	0.032
O4	0.1992 (4)	0.8494 (3)	0.9896 (2)	0.054
O5	0.1745 (3)	1.0846 (3)	0.9614 (2)	0.039
C6	0.2414 (5)	1.1369 (5)	1.0653 (3)	0.048
N1	−0.4306 (4)	0.2944 (4)	0.7031 (2)	0.033
C7	−0.5271 (5)	0.1174 (5)	0.6643 (3)	0.048
C8	−0.4317 (7)	0.0099 (6)	0.6813 (4)	0.091
C9	−0.2842 (5)	0.3696 (5)	0.6566 (3)	0.045
C10	−0.3262 (5)	0.3685 (5)	0.5458 (3)	0.055
C11	−0.3600 (5)	0.3132 (6)	0.8144 (3)	0.051
C12	−0.4878 (6)	0.2490 (7)	0.8749 (3)	0.070
C13	−0.5528 (5)	0.3761 (5)	0.6777 (3)	0.048
C14	−0.4853 (8)	0.5545 (6)	0.7094 (4)	0.084

[a] Equivalent isotropic temperature factor U_{eq} (Å^2) defined as one-third of the trace of the orthogonal U_{ij} tensor.

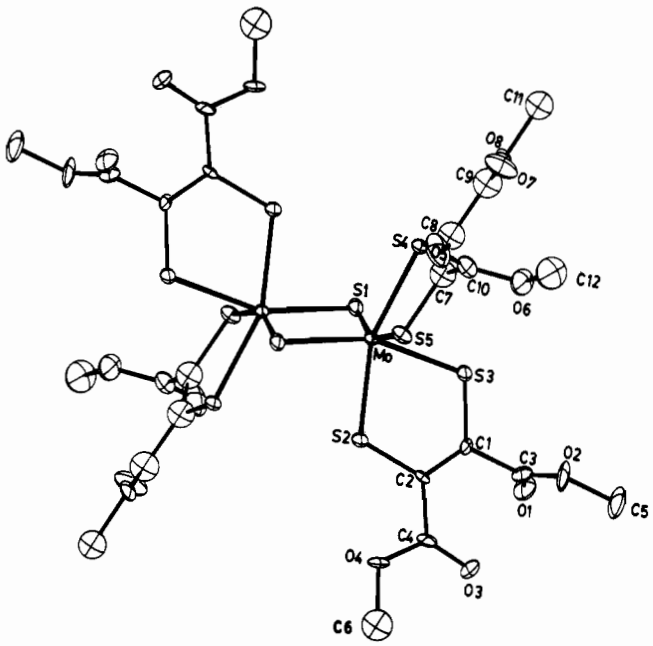

Figure 7. Structure and labeling of the $[Mo_2S_2(S_2C_2(CO_2Me)_2)_4]^{2-}$ anion in V. Thermal motion is represented by 50% probability ellipsoids as drawn by ORTEP.[56]

The cyclic voltammograms of II and III are similar, and each displays two irreversible oxidations around 1 V. A quasireversible reduction wave is observed in the voltammogram of V at −0.800 V, and an irreversible oxidation, at +0.711 V. The anodic component of the reduction wave increases in intensity as the scan rate is increased from 100 to 800 mV/s and indicates a reaction following electron transfer occurring at a rate comparable to the scan rates employed. The voltammogram of IV in CH_2Cl_2 solution shows two reversible waves at +0.020 and +0.420 V, respectively (Figure 8), that correspond to the −2/−1 and −1/0 couples. Potential step measurements show a current function ($i_a(t/C)^{1/2}$) of 10.9 for a step of +0.2 V, indicative of a one-electron process. Stepping to 0.75 V, the current function, as expected, is consistent with a two-electron step ($i_a(t/C)^{1/2}$ = 25.8). Plots of peak current vs $v^{1/2}$ are linear and confirm the reversibility of the oxidation waves. Similar behavior is observed also with the W analogue

Table IV. Fractional Atomic Coordinates and Thermal Parameters for *syn*-$[Ph_4P]_2[Mo_2O_2S_2(S_2C_2(CO_2Me)_2)_2]\cdot 2DMF$ (III)

atom	x	y	z	U^a	atom	x	y	z	U^a
Mo1	0.2616 (0)	0.3377 (0)	0.2684 (0)	0.044	C45	−0.2777 (6)	0.4905 (5)	0.0724 (4)	0.063
Mo2	0.2782 (0)	0.4913 (0)	0.1910 (0)	0.042	C46	−0.2618 (5)	0.5092 (5)	0.1474 (4)	0.053
S1	0.2360 (1)	0.4874 (1)	0.3046 (1)	0.058	C51	−0.0634 (5)	0.6345 (4)	0.3183 (4)	0.048
S2	0.3625 (1)	0.3572 (1)	0.1817 (1)	0.056	C52	−0.0747 (5)	0.6888 (5)	0.3809 (4)	0.061
S3	0.3688 (1)	0.2088 (1)	0.2859 (1)	0.056	C53	−0.0096 (7)	0.7668 (6)	0.4058 (5)	0.083
S4	0.2853 (1)	0.3393 (1)	0.3989 (1)	0.060	C54	0.0656 (7)	0.7947 (6)	0.3685 (6)	0.088
S5	0.4160 (1)	0.5388 (1)	0.1303 (1)	0.047	C55	0.0785 (6)	0.7429 (6)	0.3068 (5)	0.080
S6	0.3020 (1)	0.6512 (1)	0.2384 (1)	0.053	C56	0.0140 (6)	0.6628 (5)	0.2816 (4)	0.067
O1	0.1404 (3)	0.2877 (3)	0.2275 (3)	0.065	P2	−0.1579 (1)	0.1098 (1)	0.0789 (1)	0.042
O2	0.1644 (3)	0.4801 (3)	0.1266 (3)	0.063	C61	−0.2415 (5)	0.0252 (4)	0.0128 (4)	0.047
O3	0.4761 (5)	0.0595 (4)	0.3805 (3)	0.092	C62	−0.3372 (5)	−0.0109 (4)	0.0249 (4)	0.052
O4	0.3144 (4)	0.0320 (4)	0.4005 (3)	0.088	C63	−0.3975 (5)	−0.0805 (5)	−0.0243 (4)	0.059
O5	0.2385 (5)	0.2268 (5)	0.5194 (3)	0.132	C64	−0.3631 (6)	−0.1130 (5)	−0.0857 (4)	0.056
O6	0.3915 (4)	0.1676 (4)	0.5251 (3)	0.083	C65	−0.2677 (6)	−0.0782 (5)	−0.0982 (4)	0.064
O7	0.4452 (4)	0.7663 (4)	0.0569 (3)	0.085	C66	−0.2082 (5)	−0.0092 (5)	−0.0490 (4)	0.062
O8	0.5569 (4)	0.6600 (4)	0.0735 (3)	0.109	C71	−0.2382 (5)	0.1657 (4)	0.1332 (4)	0.042
O9	0.3051 (5)	0.8479 (4)	0.1984 (4)	0.110	C72	−0.2603 (6)	0.1268 (5)	0.1926 (4)	0.058
O10	0.4775 (4)	0.8434 (3)	0.2076 (3)	0.073	C73	−0.3302 (6)	0.1641 (5)	0.2316 (4)	0.067
C1	0.3560 (5)	0.1756 (5)	0.3695 (4)	0.049	C74	−0.3794 (5)	0.2402 (5)	0.2098 (5)	0.064
C2	0.3204 (5)	0.2315 (5)	0.4181 (4)	0.053	C75	−0.3580 (5)	0.2797 (5)	0.1516 (4)	0.061
C3	0.3910 (6)	0.0849 (5)	0.3837 (4)	0.058	C76	−0.2870 (5)	0.2425 (5)	0.1120 (4)	0.054
C4	0.3437 (7)	−0.0563 (6)	0.4230 (7)	0.122	C81	−0.0584 (5)	0.0564 (4)	0.1389 (4)	0.045
C5	0.3099 (6)	0.2085 (6)	0.4922 (4)	0.069	C82	0.0039 (5)	0.1077 (4)	0.2003 (4)	0.053
C6	0.3871 (8)	0.1395 (7)	0.5946 (5)	0.114	C83	0.0861 (5)	0.0706 (5)	0.2457 (4)	0.064
C7	0.4204 (4)	0.6577 (4)	0.1368 (4)	0.043	C84	0.1038 (6)	−0.0188 (6)	0.2285 (5)	0.075
C8	0.3732 (5)	0.7047 (4)	0.1834 (4)	0.045	C85	0.0412 (7)	−0.0710 (5)	0.1683 (5)	0.073
C9	0.4752 (6)	0.7020 (5)	0.0855 (4)	0.057	C86	−0.0408 (6)	−0.0343 (5)	0.1221 (4)	0.056
C10	0.6098 (8)	0.6921 (6)	0.0195 (6)	0.135	C91	−0.0926 (5)	0.1868 (4)	0.0317 (3)	0.044
C11	0.3807 (6)	0.8061 (5)	0.1966 (4)	0.057	C92	−0.1531 (5)	0.2212 (5)	−0.0296 (4)	0.051
C12	0.4911 (7)	0.9416 (5)	0.2130 (6)	0.101	C93	−0.1034 (6)	0.2799 (5)	−0.0665 (4)	0.062
P1	−0.1411 (1)	0.5277 (1)	0.2896 (1)	0.045	C94	0.0048 (7)	0.3064 (5)	−0.0435 (4)	0.069
C21	−0.0716 (5)	0.4414 (5)	0.3335 (4)	0.046	C95	0.0632 (5)	0.2729 (5)	0.0175 (4)	0.062
C22	−0.0981 (5)	0.3496 (5)	0.3049 (4)	0.056	C96	0.0159 (5)	0.2138 (4)	0.0543 (4)	0.052
C23	−0.0497 (6)	0.2849 (5)	0.3429 (5)	0.068	N110	0.3152 (5)	0.6910 (5)	0.5050 (4)	0.085
C24	0.0238 (6)	0.3067 (6)	0.4079 (5)	0.071	O111	0.2547 (7)	0.7848 (6)	0.5807 (5)	0.225
C25	0.0507 (6)	0.3951 (6)	0.4358 (4)	0.065	C112	0.3307 (10)	0.7592 (9)	0.5582 (7)	0.143
C26	0.0024 (5)	0.4637 (5)	0.3993 (4)	0.054	C113	0.4022 (10)	0.6737 (9)	0.4721 (7)	0.157
C31	−0.2668 (5)	0.5337 (5)	0.3150 (4)	0.049	C114	0.2181 (7)	0.6304 (7)	0.4851 (5)	0.109
C32	−0.3222 (6)	0.6095 (5)	0.3049 (4)	0.069	N120	0.1303 (20)	0.0057 (15)	0.6338 (13)	0.194
C33	−0.4220 (6)	0.6112 (7)	0.3219 (5)	0.083	N130	0.2364 (19)	0.1586 (15)	0.7943 (12)	0.135
C34	−0.4639 (6)	0.5377 (9)	0.3488 (5)	0.092	O121	0.1827 (8)	0.1157 (9)	0.7295 (7)	0.237
C35	−0.4095 (7)	0.4631 (8)	0.3572 (5)	0.100	O131	0.2010 (7)	0.0450 (7)	0.6973 (6)	0.171
C36	−0.3096 (6)	0.4597 (6)	0.3416 (5)	0.078	C123	0.0643 (26)	−0.0307 (21)	0.6023 (17)	0.206
C41	−0.1638 (5)	0.4995 (4)	0.1926 (4)	0.046	C124	0.1670 (25)	−0.0431 (23)	0.6114 (17)	0.235
C42	−0.0808 (5)	0.4686 (5)	0.1622 (4)	0.054	C133	0.2142 (26)	0.2207 (25)	0.8320 (19)	0.330
C43	−0.0966 (6)	0.4531 (5)	0.0870 (4)	0.060	C134	0.2824 (30)	0.1705 (24)	0.8006 (19)	0.281
C44	−0.1935 (7)	0.4632 (5)	0.0423 (4)	0.063					

[a] Equivalent isotropic temperature factor U_{eq} (Å^2) defined as one-third of the trace of the orthogonal U_{ij} tensor.

of IV. The latter shows two reversible oxidation waves at −0.05 and +0.42 V.

Description of the Structures

$[Et_4N]_2[MoO(S_2C_2(CO_2Me)_2)_2]$ (I). In this structure, a disorder problem associated with one of the Et_4N^+ cations was resolved successfully. The structure of the other cation was unexceptional. Both cations in the asymmetric unit are well separated from the anion and will not be considered further. The structure of the $[MoO(S_2C_2(CO_2Me)_2)_2]^{2-}$ anion and the numbering scheme are shown in Figure 3. Selected structural parameters are shown in Table VII. The Mo(IV) ion is square-pyramidal coordinated by two dithiolene bidentate ligands that occupy the equatorial positions of the distorted square pyramid. A terminal axial oxo ligand completes the coordination sphere. The Mo atom is elevated from the equatorial plane defined by the S atoms by 0.71 Å. Monomeric Mo(IV) five-coordinate complexes are quite rare. The structure of the anion in I closely resembles the structure of the $[MoO(S_4)_2]^{2-}$ anion.[3] In the latter the Mo=O bond at 1.685 (7) Å is nearly identical in length with that in I at 1.686 (6) Å. The unequal Mo–S bonds in $[MoO(S_4)_2]^{2-}$ at 2.363 (2) and 2.395 (2) Å have a mean value (2.379 (2) Å) similar to the corresponding value for I at 2.380 (2) Å. The O_{ax}–Mo–S_{eq} angles also are very similar at 108.7 and 108.9°, respectively, in $[MoO(S_4)_2]^{2-}$ and I. An examination of the rectangle of sulfur donors in the

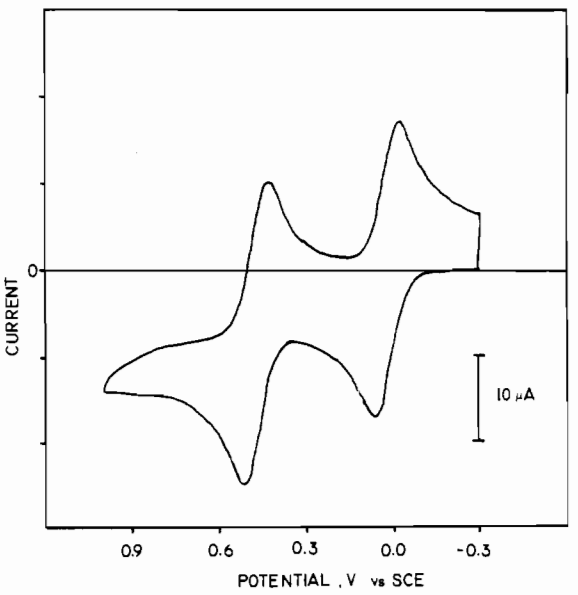

Figure 8. Cyclic voltammetry trace of the $[Ph_4P]_2[Mo(S_2C_2(CO_2Me)_2)_3]\cdot DMF\cdot C_6H_6$ (IV) complex in CH_2Cl solution.

Table V. Fractional Atomic Coordinates and Thermal Parameters for $[Ph_4P]_2[Mo(S_2C_2(CO_2Me)_2)_3]\cdot DMF\cdot C_6H_6$ (IV)

atom	x	y	z	U_{eq}[a]	atom	x	y	z	U_{eq}[a]
Mo	−0.01734 (8)	0.4772 (1)	0.61918 (4)	0.0205 (4)	C11A	0.442 (1)	0.448 (2)	0.4658 (6)	0.062 (7)
S1	−0.0917 (2)	0.4850 (4)	0.6538 (1)	0.032 (1)	C12A	0.409 (1)	0.470 (2)	0.4903 (5)	0.054 (6)
S2	−0.0993 (2)	0.4207 (4)	0.5866 (1)	0.030 (1)	C13A	0.3237 (9)	0.324 (1)	0.5528 (4)	0.023 (4)
S3	0.0306 (2)	0.3401 (4)	0.6053 (1)	0.029 (1)	C14A	0.3722 (9)	0.270 (1)	0.5617 (4)	0.029 (5)
S4	0.0430 (2)	0.4494 (3)	0.6659 (1)	0.026 (1)	C15A	−0.1323 (9)	0.692 (1)	0.5794 (5)	0.036 (5)
S5	0.0039 (2)	0.6328 (4)	0.6335 (1)	0.030 (1)	C16A	−0.187 (1)	0.664 (1)	0.5872 (5)	0.036 (5)
S6	0.0092 (2)	0.5330 (4)	0.5708 (1)	0.030 (1)	C17A	−0.2362 (9)	0.717 (1)	0.5776 (5)	0.039 (5)
O1	−0.2197 (6)	0.501 (1)	0.6724 (3)	0.056 (4)	C18A	0.2684 (9)	0.296 (1)	0.5605 (4)	0.034 (5)
O2	−0.2341 (7)	0.361 (1)	0.6534 (3)	0.054 (4)	C19A	0.3680 (8)	0.513 (1)	0.5563 (4)	0.027 (4)
O3	−0.2632 (8)	0.441 (1)	0.5907 (4)	0.072 (5)	C20A	0.357 (1)	0.396 (2)	0.0497 (5)	0.044 (6)
O4	−0.2162 (7)	0.332 (1)	0.5688 (4)	0.058 (4)	C21A	0.613 (1)	0.630 (2)	0.4319 (5)	0.042 (5)
O5	0.0664 (6)	0.134 (1)	0.6308 (3)	0.043 (3)	C22A	0.425 (1)	0.355 (2)	0.0918 (5)	0.045 (6)
O6	0.1541 (6)	0.2032 (9)	0.6314 (3)	0.040 (3)	C23A	0.438 (1)	0.445 (2)	0.0971 (5)	0.043 (6)
O7	0.1251 (6)	0.225 (1)	0.6941 (3)	0.049 (4)	C24A	0.4082 (9)	0.512 (1)	0.0794 (4)	0.034 (5)
O8	0.1163 (6)	0.362 (1)	0.7146 (3)	0.047 (4)	C25A	0.2655 (8)	0.466 (1)	0.2266 (4)	0.023 (4)
O9	−0.0017 (6)	0.845 (1)	0.6144 (3)	0.050 (4)	C26A	0.247 (1)	0.447 (1)	0.2544 (5)	0.040 (5)
O10	0.0865 (7)	0.814 (1)	0.6028 (3)	0.051 (4)	C27A	0.190 (1)	0.420 (2)	0.2574 (5)	0.051 (6)
O11	0.5194 (8)	0.287 (1)	0.5430 (4)	0.077 (5)	C28A	−0.155 (1)	0.596 (2)	0.7696 (6)	0.057 (7)
O12	0.0430 (7)	0.657 (1)	0.5232 (4)	0.060 (4)	C29A	0.169 (1)	0.423 (2)	0.2017 (5)	0.053 (6)
C1	−0.1579 (9)	0.444 (1)	0.6363 (5)	0.035 (5)	C30A	0.2261 (9)	0.455 (1)	0.2008 (5)	0.038 (5)
C2	−0.1625 (8)	0.419 (1)	0.6065 (4)	0.020 (4)	C31A	0.3801 (9)	0.410 (1)	0.2077 (4)	0.027 (5)
C3	0.0709 (9)	0.298 (1)	0.6372 (4)	0.029 (5)	C32A	0.560 (1)	0.406 (2)	0.2852 (5)	0.051 (6)
C4	0.0777 (7)	0.344 (1)	0.6649 (4)	0.017 (4)	C33A	0.471 (1)	0.335 (2)	0.2023 (6)	0.065 (7)
C5	0.0214 (9)	0.692 (1)	0.6009 (4)	0.028 (5)	C34A	0.444 (1)	0.270 (2)	0.1838 (5)	0.048 (6)
C6	0.0216 (6)	0.651 (1)	0.5750 (4)	0.026 (4)	C35A	0.616 (1)	0.273 (2)	0.3230 (5)	0.054 (6)
C7	−0.2084 (9)	0.441 (2)	0.6559 (5)	0.036 (5)	C36A	0.6476 (9)	0.345 (1)	0.3099 (5)	0.035 (5)
C8	−0.282 (1)	0.347 (2)	0.6741 (6)	0.083 (8)	C37A	0.3766 (9)	0.541 (2)	0.2584 (5)	0.039 (5)
C9	−0.220 (1)	0.398 (2)	0.5891 (5)	0.041 (8)	C38A	0.394 (1)	0.630 (2)	0.2623 (6)	0.059 (6)
C10	−0.272 (1)	0.312 (2)	0.5505 (7)	0.084 (8)	C39A	0.423 (1)	0.660 (2)	0.2897 (6)	0.064 (7)
C11	0.096 (1)	0.203 (1)	0.6326 (4)	0.031 (5)	C40A	0.439 (1)	0.596 (2)	0.3120 (5)	0.054 (6)
C12	0.180 (1)	0.112 (2)	0.6321 (5)	0.047 (6)	C41A	0.4223 (9)	0.510 (2)	0.3073 (5)	0.043 (5)
C13	0.1097 (9)	0.302 (2)	0.6916 (5)	0.036 (5)	C42A	0.2908 (9)	0.479 (1)	0.2816 (5)	0.036 (5)
C14	0.143 (1)	0.325 (2)	0.7434 (6)	0.063 (7)	C43A	0.3379 (9)	0.5989 (1)	0.1962 (4)	0.027 (5)
C15	0.032 (1)	0.790 (2)	0.6066 (5)	0.039 (5)	C44A	0.293 (1)	0.660 (2)	0.1966 (5)	0.043 (5)
C16	0.101 (1)	0.911 (2)	0.6053 (6)	0.063 (7)	C45A	−0.205 (1)	0.756 (2)	0.6807 (5)	0.052 (6)
C17	0.031 (1)	0.707 (2)	0.5462 (6)	0.049 (6)	C46A	−0.157 (1)	0.742 (2)	0.6655 (6)	0.057 (6)
C18	0.047 (1)	0.703 (2)	0.4940 (8)	0.100 (9)	C47A	0.387 (1)	0.695 (2)	0.1628 (5)	0.042 (6)
P1	0.6688 (3)	0.4273 (4)	−0.0320 (1)	0.040 (1)	C48A	0.385 (1)	0.615 (1)	0.1794 (5)	0.039 (5)
P2	0.3391 (2)	0.5030 (4)	0.2220 (1)	0.041 (1)	C18	0.248 (1)	0.374 (2)	0.1180 (5)	0.053 (6)
C1A	0.2594 (8)	0.465 (1)	0.5188 (4)	0.021 (4)	C28	0.189 (1)	0.385 (2)	0.1151 (6)	0.072 (7)
C2A	0.235 (1)	0.449 (1)	0.4901 (5)	0.039 (5)	C38	0.168 (1)	0.474 (2)	0.1167 (5)	0.059 (6)
C3A	0.177 (1)	0.468 (2)	0.4813 (5)	0.055 (6)	C48	0.203 (1)	0.545 (2)	0.1201 (5)	0.061 (7)
C4A	0.141 (1)	0.502 (2)	0.5024 (5)	0.049 (6)	C58	0.265 (1)	0.533 (2)	0.1220 (5)	0.051 (6)
C5A	0.165 (1)	0.524 (2)	0.5312 (5)	0.058 (6)	C68	0.286 (1)	0.448 (2)	0.1221 (5)	0.047 (6)
C6A	0.225 (1)	0.505 (1)	0.5395 (5)	0.043 (5)	C2S	0.027 (1)	0.384 (2)	0.2761 (7)	0.078 (8)
C7A	0.3732 (9)	0.403 (1)	0.5004 (4)	0.030 (5)	OS	0.024 (1)	0.295 (2)	0.2680 (7)	0.062 (9)
C8A	0.365 (1)	0.319 (2)	0.4847 (6)	0.054 (6)	NSb	0	0.430 (3)	0.250	0.118 (13)
C9A	0.400 (1)	0.300 (2)	0.4601 (6)	0.062 (7)	C1S	0	0.503 (5)	0.250	0.186 (28)
C10A	0.434 (1)	0.366 (2)	0.4511 (5)	0.058 (6)					

[a] Equivalent isotropic temperature factor U_{eq} (Å^2) defined as one-third of the trace of the orthogonal U_{ij} tensor.

equatorial plane shows that the closest S–S distances in I are intramolecular contacts within the dithiolene ligands at 3.157 (3) Å. Interligand contacts are slightly longer at a distance of 3.227 (3) Å. The reverse situation prevails in the structure of $[MoO(S_4)_2]^{2-}$, where the interligand S–S contacts at 2.990 (3) Å are significantly shorter than the intraligand contacts at 3.376 (3) Å. This difference in the geometry of the S_{eq} rectangles can be attributed to differences in the intraligand S–S distance ("bite") between the S_4^{2-} and $[S_2C_2(CO_2Me)_2]^{2-}$ ligands (at 3.376 (3) and 3.15 (1) Å, respectively) and an apparent tendency of the $[OMoS_4]$ unit to maintain the Mo–S bond length at 2.38 Å and the O_{ax}–Mo–S_{eq} angle at ~109°. The sum of the S_{eq}–Mo–S_{eq} angles in I at 335.8° is very similar to that in the $[MoO(S_4)_2]^{2-}$ anion (336.5°) although in the latter the S_{eq}–Mo–S_{eq} angles are found in two widely different sets of 77.86° (interligand) and 90.40° (intraligand). One of the two dithiolene ligands in I is positionally disordered. The intraligand distances and angles are unexceptional and will not be discussed further.

$[Ph_4P]_2$[*syn*-$\{Mo_2(O)_2(\mu\text{-}S)_2\}(\eta^1\text{-}S\text{-}\eta^1\text{-}SC_2(CO_2Me)_2)_2$] (III) and $[Et_4N]_2$[*anti*-$\{Mo_2(O)_2(\mu\text{-}S)_2\}(\eta^1\text{-}S\text{-}\eta^1\text{-}SC_2(CO_2Me)_2)_2$] (II). The anion in II is located on a center of symmetry and is required to possess a planar Mo_2S_2 unit; the anion in III is found on a general position with no crystallographically imposed symmetry. The idealized symmetries of the $[Mo_2O_2S_2]^{2+}$ cores in II and III are C_{2h} and C_{2v}, respectively. The coordination geometries around each of the Mo atoms in both II and III are distorted square pyramidal and quite similar to the geometry of the same unit in I with the axial positions occupied by terminal oxo groups and the equatorial positions by two bridging sulfides and the S atoms of the dithiolene ligands (Figures 4 and 5). Structural parameters for II and III are shown in Table VII and a comparison of II and III to the *anti*- and *syn*-$[Mo_2S_4(S_2C_2H_4)_2]^{2-}$ complexes[37,38] is presented in Table IX. The Mo–S_b distances in II and III at 2.328 (1) and 2.331 (3) Å, respectively, are very similar to an unweighted average value of 2.32 (2) Å reported for numerous other structures that contain bis(μ-sulfido)-bridged binuclear Mo(V) complexes.[38] For the latter, the apparent invariability in the Mo–S_b distances[39] and the Mo–S_b–Mo angles[40] (~76°) have

(37) Bunzey, G.; Enemark, J. H.; Howie, J. K.; Sawyer, D. T. *J. Am. Chem. Soc.* **1977**, *99*, 4168.
(38) Bunzey, G.; Enemark, J. H. *Inorg. Chem.* **1978**, *17*, 682.
(39) Ricard, L.; Estienne, J.; Weiss, R. *Inorg. Chem.* **1973**, *12*, 2183.
(40) Dahl, L. F.; Frisch, P. D.; Gust, G. R. In *Proceedings of the Climax First International Symposium on Chemistry and Uses of Molybdenum*; Mitchell, P. C. H., Ed.; Climax Molybdenum Co.: London, 1973; p 134.

Table VI. Fractional Atomic Coordinates and Thermal Parameters for $[Ph_4P]_2[Mo_2S_2(S_2C_2(CO_2Me)_2)_4]\cdot 2CH_2Cl_2$ (V)

atom	x	y	z	U^a
Mo	0.5198 (1)	0.9192 (1)	0.0443 (1)	0.026
S1	0.5133 (3)	1.0885 (2)	0.1273 (2)	0.034
S2	0.3512 (3)	0.8602 (2)	0.1031 (2)	0.036
S3	0.4571 (3)	0.7165 (2)	−0.0292 (2)	0.042
S4	0.6984 (3)	0.9212 (2)	0.0112 (2)	0.037
S5	0.6248 (3)	0.9369 (2)	0.2168 (2)	0.049
P1	0.2435 (3)	0.4008 (2)	0.3540 (2)	0.039
C1	0.3373 (10)	0.6564 (8)	0.0076 (8)	0.031
C2	0.2906 (11)	0.7162 (9)	0.0675 (9)	0.035
C3	0.2849 (11)	0.5273 (9)	−0.0410 (10)	0.040
C4	0.1873 (11)	0.6592 (11)	0.0970 (9)	0.043
C5	0.2814 (13)	0.3623 (9)	−0.0218 (12)	0.078
C6	0.0430 (15)	0.6819 (13)	0.1722 (12)	0.089
C7	0.7522 (7)	0.9284 (6)	0.2069 (5)	0.038
C8	0.7856 (7)	0.9216 (6)	0.1197 (5)	0.041
C9	0.9001 (7)	0.9160 (6)	0.1182 (5)	0.047
C10	0.8251 (7)	0.9337 (6)	0.3052 (5)	0.065
C11	1.0140 (7)	0.8707 (6)	0.0049 (5)	0.072
C12	0.8913 (16)	0.8292 (17)	0.3899 (16)	0.149
O1	0.2182 (3)	0.4800 (3)	−0.1241 (3)	0.052
O2	0.3275 (3)	0.4835 (3)	0.0171 (3)	0.064
O3	0.1415 (3)	0.5589 (3)	0.0766 (3)	0.060
O4	0.1492 (3)	0.7305 (3)	0.1472 (3)	0.069
O5	0.8793 (3)	1.0199 (3)	0.3775 (3)	0.089
O6	0.8191 (3)	0.8346 (3)	0.3040 (3)	0.082
O7	0.9731 (3)	0.9369 (3)	0.1899 (3)	0.088
O8	0.9051 (3)	0.8793 (3)	0.0206 (3)	0.055
CC1	0.7434 (3)	0.5181 (3)	0.5163 (3)	0.041
CC2	0.8354 (3)	0.5503 (3)	0.4735 (3)	0.064
CC3	0.8234 (14)	0.4902 (12)	0.3698 (12)	0.086
CC4	0.7182 (14)	0.4040 (11)	0.3112 (11)	0.071
CC5	0.6314 (13)	0.3712 (11)	0.3522 (11)	0.070
CC6	0.6414 (12)	0.4320 (10)	0.4552 (10)	0.060
CC7	0.3462 (11)	0.4930 (9)	0.3068 (9)	0.047
CC8	0.3450 (12)	0.5971 (9)	0.3164 (9)	0.055
CC9	0.4260 (13)	0.6702 (10)	0.2858 (9)	0.061
CC10	0.5036 (13)	0.6386 (10)	0.2442 (10)	0.063
CC11	0.5062 (13)	0.5354 (11)	0.2342 (10)	0.069
CC12	0.4237 (12)	0.4624 (10)	0.2643 (10)	0.060
CC13	0.9033 (10)	0.6534 (8)	0.7225 (8)	0.034
CC14	0.9843 (11)	0.7443 (9)	0.7138 (8)	0.046
CC15	1.1004 (12)	0.7818 (9)	0.7686 (9)	0.052
CC16	1.1349 (21)	0.7332 (17)	0.8285 (16)	0.068
CC17	1.0464 (14)	0.6369 (11)	0.8431 (10)	0.058
CC18	0.9320 (11)	0.5994 (9)	0.7876 (8)	0.046
CC19	0.2770 (11)	0.2843 (8)	0.3536 (8)	0.041
CC20	0.2561 (11)	0.1999 (9)	0.2640 (9)	0.049
CC21	0.2840 (12)	0.1112 (10)	0.2627 (10)	0.065
CC22	0.3328 (13)	0.1027 (11)	0.3491 (11)	0.072
CC23	0.3529 (13)	0.1881 (12)	0.4442 (11)	0.080
CC24	0.3284 (11)	0.2799 (9)	0.4477 (9)	0.051
C	0.7383 (24)	0.1749 (20)	0.4770 (18)	0.140
Cl1	0.8253 (21)	0.2709 (19)	0.5016 (16)	0.140
Cl2	0.1347 (24)	0.6769 (16)	0.4673 (19)	0.140
Cl3	0.8917 (21)	0.2896 (20)	0.5498 (17)	0.140
Cl4	0.6246 (21)	0.1262 (17)	0.4804 (14)	0.140
Cl5	0.3662 (22)	0.8759 (17)	0.4671 (15)	0.140
Cl6	0.7415 (19)	0.1476 (14)	0.5629 (14)	0.140

[a] Equivalent isotropic temperature factor U_{eq} (Å^2) defined as one-third of the trace of the orthogonal U_{ij} tensor.

been noted previously. The Mo–S_b–Mo angles in II and III are 77.13 (1) and 75.5 (1)°, respectively. The Mo–Mo distances in II and III at 2.904 (1) and 2.853 (1) Å are within the range reported previously for similar complexes[38] (2.79 (1)–2.920 (1) Å). In the $[Mo_2S_4(S_2C_2H_4)_2]^{2-}$ syn and anti complexes, the Mo–Mo distances differ by only 0.015 Å.[38] The difference between II and III of 0.05 Å is significant and more in accord with the electronic structure and bonding interactions within the *syn*- and *anti*-$[Mo_2E_2S_2]^{2+}$ units (E = S, O). For the Mo_2S_4 units the greater stability of the syn isomers has been attributed to a greater Mo–Mo 4d overlap population. The calculated Mulliken charge analysis, by the Fenske–Hall method, shows populations of 0.087 and 0.061 for the syn and anti isomers, respectively.[41] It has been suggested that this weak metal–metal bonding is sufficient to explain the diamagnetic behavior of the dimers without invoking a strong antiferromagnetic coupling mechanism.[41]

$[Ph_4P]_2[Mo(S_2C_2(CO_2Me)_2)_3]$ (IV). In this structure, the Ph_4P^+ cations are well separated from the anion and are unexceptional. A brief account of the cation structural parameters is given as a footnote in Table VIII. The anion in IV (Figure 6) occupies a general position in the monoclinic ($C2/c$) unit cell. The Mo(IV) atom is coordinated by three bidentate 1,2-dicarbomethoxy-1,2-ethylenedithiolate ligands in a structure where the polyhedron of sulfur atoms defines a slightly distorted trigonal prismatic arrangement. The central Mo atom is located 0.90, 0.91, and 0.92 Å from the centers of the rectangular $S_1S_2S_3S_4$, $S_3S_4S_5S_6$, and $S_1S_2S_5S_6$ faces, respectively. An analysis of the polyhedron geometry after Muetterties and Guggenberger[42] shows the following parameters: The dihedral angles (δ) for the S_6 polyhedron trigonal faces are 11.67, 15.36, and 19.70° at b_1 and 120.33, 119.84, and 119.08° at b_2. The angles for the remaining edges range from 87.0 to 93.0°. The δ's for the idealized trigonal prismatic structure, defined as the dihedral angles formed by the normals to adjacent polytopal faces,[42] are 0° for the b_1 angles, 120° for the b_2 angles, and 90° for the rest of the edges of the polyhedron (Figure 6B). The δ's for the octahedron edges are all 70.5°. The mean value of the S–Mo–S interligand trans angles of 135° is very close to the average value of 136° found for the trans angles in the $Re(S_2C_2(C_6H_5)_2)_3$,[43] $V(S_2C_2(C_6H_5)_2)_3$,[44] $Mo(S_2C_2H_2)_3$,[45] $Mo(S_2C_6H_4)_3$,[46] and $[Nb(S_2C_6H_4)_3]^-$[45] complexes. The Mo–S bond length in IV at 2.393 (6) Å is somewhat longer than the Mo–S bond in the $Mo(S_2C_2H_2)_3$[45] and $Mo(S_2C_6H_4)_3$[46] complexes at 2.33 (1) and 2.367 (2) Å, respectively, similar to that in the $[Mo(S_2C_2(CN)_2)_3]^{2-}$ anion[47] at 2.373 Å, and identical with that in tris(quinoxaline-2,3-dithiolato)molybdate(IV) at 2.393 Å.[48] The geometry of the anion in IV is similar to that found in the recently reported structure of the analogous W/Se complex[25] and appreciably different from that found in the $[Mo(S_2C_2(CN)_2)_3]^{2-}$ anion.[47] The S_6 polyhedron in the latter is halfway between octahedral and trigonal prismatic geometry. The difference may arise from differences in the relative energies of the Mo(IV) d orbitals and the appropriate ligand orbitals.[46] It has been suggested, on the basis of σ-bonding arguments, that for highly covalent second- and third-row transition-metal complexes with the d^0, d^1, and d^2 electronic configurations, the trigonal prismatic geometry is preferred.[49] As observed previously in the structure of the $(Ph_4P)_2Fe_2[S_2C_2(COOCH_3)_2]_4$ complex,[50] the MS_2C_2 rings in IV are planar with one of the two carboxylate groups lying in this metal–ligand plane and the other nearly perpenticular to it.

$[Ph_4P]_2[Mo_2S_2(S_2C_2(CO_2Me)_2)_4]\cdot 2CH_2Cl_2$ (V). The centrosymmetric anion in this compound (Figure 7) contains a central core of two edge-sharing MoS_6 distorted octahedra. The coordination sphere around each of the two Mo atoms contains four sulfur atoms contributed by the two bidentate dithiolene ligands and the two μ_2-S ligands. The MoS_6 units display distorted octahedral geometry not unlike the one observed in the structure of the corresponding W/Se complex.[25] The dithiolene Mo–S bonds range from 2.377 (3) to 2.466 (4) Å and are clearly separated into two pairs. The two long distances, one on each of the two

(41) Chandler, T.; Litchtenberger, D. L.; Enemark, J. H. *Inorg. Chem.* **1981**, *20*, 75.
(42) Muetterties, E. L.; Guggenberger, L. J. *J. Am. Chem. Soc.* **1974**, *96*, 1748.
(43) Eisenberg, R.; Ibers, J. A. *Inorg. Chem.* **1966**, *5*, 411.
(44) (a) Eisenberg, R.; Stiefel, E. I.; Rosenberg, R. C.; Gray, H. B. *J. Am. Chem. Soc.* **1966**, *88*, 2874. (b) Eisenberg, R.; Gray, H. B. *Inorg. Chem.* **1967**, *6*, 1844.
(45) Smith, A. E.; Schrauzer, G. N.; Mayweg, V. P.; Heinrich, W. *J. Am. Chem. Soc.* **1965**, *87*, 5798.
(46) Bennett, M. J.; Cowie, M.; Martin, J. L.; Takats, J. *J. Am. Chem. Soc.* **1973**, *95*, 7504.
(47) Brown, G. F.; Stiefel, E. I. *Inorg. Chem.* **1973**, *12*, 2140.
(48) Huisman, R.; DeJonge, R.; Haas, C.; Jellinek, F. *J. Solid State Chem.* **1971**, *3*, 56.
(49) Boyde, S.; Garner, C. D.; Enemark, J. H.; Ortega, R. B. *Polyhedron* **1986**, *5*, 377.
(50) Kanatzidis, M. G.; Coucouvanis, D. *Inorg. Chem.* **1984**, *23*, 403.

Table VII. Summary of Interatomic Distances (Å) and Angles (deg) for $[Et_4N]_2[MoO(S_2C_2(CO_2Me)_2)_2]$ (I), *anti*-$[Et_4N]_2[Mo_2O_2S_2(S_2C_2(CO_2Me)_2)_2]$ (II), *syn*-$[Ph_4P]_2[Mo_2O_2S_2(S_2C_2(CO_2Me)_2)_2]\cdot 2DMF$ (III), $[Ph_4P]_2[Mo(S_2C_2(CO_2Me)_2)_3]\cdot DMF\cdot C_6H_6$ (IV), and $[Ph_4P]_2[Mo_2S_2(S_2C_2(CO_2Me)_2)_4]\cdot 2CH_2Cl_2$ (V)

	I	II	III	IV	V
			Distances[a,b]		
Mo–Mo[a]		2.904 (1)	2.853 (1)		2.938 (1)
Mo–S_b		2.328	2.331 (4, 3)		2.321
range		2.327 (1), 2.330 (1)	2.327 (3)–2.341 (3)		2.319 (3)–2.323 (3)
Mo–S	2.380 (4, 4)	2.419	2.425 (4, 8)	2.393 (6, 5)	2.383,[c] 2.459[d]
range	2.370 (2)–2.388 (2)	2.425 (1), 2.413 (1)	2.408 (3)–2.443 (3)	2.384 (5)–2.397 (5)	2.388 (4), 2.378 (3)[c] 2.466 (3), 2.452 (3)[d]
Mo=O	1.686 (6)	1.684 (2)	1.675		
range			1.677 (6), 1.671 (6)		
C–S	1.758 (4, 9)	1.751	1.74 (4, 1)	1.74 (6, 2)	1.732,[c] 1.697[d]
range	1.747 (9)–1.769 (8)	1.739 (4), 1.764 (4)	1.735 (11)–1.759 (9)	1.72 (2)–1.76 (2)	1.729 (8), 1.734 (11)[c] 1.695 (8), 1.698 (12)[d]
C=C	1.32	1.338 (5)	1.349	1.35 (3, 2)	1.34
range	1.33 (1), 1.31 (1)		1.344 (14), 1.353 (14)	1.31 (2)–1.37 (2)	1.33 (2), 1.35 (2)
C–$COOCH_3$	1.47 (4, 2)	1.498	1.49 (4, 2)	1.49 (6, 3)	1.50 (2)
range	1.45 (1)–1.50 (2)	1.477 (5), 1.510 (5)	1.48 (2)–1.51 (2)	1.48 (2)–1.53 (3)	1.46 (2)–1.55 (2)
C=O	1.21 (4, 3)	1.197	1.19 (4, 2)	1.191 (6, 2)	1.19 (4, 1)
range	1.19 (3)–1.22 (3)	1.186 (4), 1.208 (4)	1.18 (2)–1.20 (1)	1.18 (2)–1.21 (2)	1.15 (1)–1.22 (1)
C–OCH_3	1.29 (4, 4)	1.34	1.31 (4, 1)	1.32 (6, 2)	1.31 (4, 1)
range	1.22 (2)–1.33 (4)	1.34 (5), 1.34 (4)	1.29 (1)–1.34 (1)	1.29 (2)–1.35 (2)	1.29 (1)–1.33 (1)
O–CH_3	1.48 (4, 4)	1.447	1.45 (4, 2)	1.44 (6, 2)	1.45 (4, 2)
range	1.44 (1)–1.54 (2)	1.443 (4), 1.452 (5)	1.43 (2)–1.46 (1)	1.42 (2)–1.45 (2)	1.43 (2)–1.48 (1)
			Angles		
Mo–S_b–Mo		77.13 (1)	75.5		78.6 (1)
range			75.3 (1), 75.6 (1)		
S_b–Mo–S_b		102.91 (1)	100.9		101.4 (1)
range			100.7 (1), 101.1 (1)		
S–Mo–S (intraligand)	83.1	81.44 (1)	81.2	80.7 (3, 2)	80.1
range	83.1 (1), 83.0 (1)		80.8 (1), 81.6 (1)	80.2 (2)–80.6 (2)	80.2 (1), 79.9 (1)
S–Mo–S (interligand, cis)	84.8			82.9 (5, 10)	84.1
range	84.3 (1), 85.3 (1)			80.7 (2)–85.9 (2)	83.1 (1), 85.1 (1)
				127.4 (3, 14)	
				124.9 (2)–129.7 (2)	
S–Mo–S (interligand, trans)	142.1			142.7 (3, 10)	156.4 (1)
range	140.7 (1), 143.5 (1)			141.0 (3)–144.1 (3)	
S_b–Mo–S (cis)		79.92 (1)	79.1 (4, 7)		78.6 (1), 86.2 (1)
range			78.0 (1)–80.7 (1)		
S_b–Mo–S (trans)		146.63 (1)	144.4 (4, 19)		
range			139.7 (1)–148.8 (1)		
S–Mo–O	108.9 (4, 5)	106.45 (2)	105.5 (4, 12)		
range	108.2 (2)–110.0 (2)	105.54 (2)–107.26 (2)	102.8 (2)–108.5 (3)		
S_b–Mo–O		104.43 (1)	108.2 (4, 9)		
range			105.6 (2)–110.3 (3)		

[a] Mean values of crystallographically independent, chemically equivalent structural parameters. The first number in parentheses represents the number of chemically equivalent bond lengths or angles averaged out; the second number represents the larger of the indiviual standard deviations or the standard deviation from the mean, σ. $\sigma = (\sum_{i=1}^{N}(x-\bar{x})^2/N(N-1))^{1/2}$. [b] In I, for cation N1, the N–C bonds are in the range 1.51 (1)–1.52 (1) Å with a mean value of 1.51 (1) Å. The C–C bonds are in the range 1.48 (1)–1.54 (1) Å with a mean of 1.52 (1) Å. For cation N2, the N–C bonds are in the range 1.48 (5)–1.66 (4) with a mean of 1.56 (5) Å. The C–C bonds are within the range 1.49 (3)–1.80 (6) with a mean value of 1.56 (6) Å. In II, for cation N1, the N–C bonds are within the range 1.519 (5)–1.526 (5) Å with a mean value of 1.52 (1) Å. The C–C bonds are within the range 1.506 (6)–1.510 (6) Å with a mean value of 1.51 (1) Å. For III, cation P1, P–C range = 1.78 (1)–1.80 (1) Å, mean P–C = 1.79 (4) Å, C–C range = 1.35 (2)–1.41 (2) Å, mean C–C = 1.38 (24, 2) Å. For cation P2, P–C range = 1.79 (1)–1.80 (1) Å, mean P–C = 1.80 (1) = C–C range = 1.36 (2)–1.42 (2) Å, mean C–C = 1.39 (24, 2) Å. For V, cation P1, P–C range = 1.78 (1)–1.82 (1) Å, mean P–C = 1.79 (2) Å, C–C range = 1.31 (2)–1.50 (3) Å, mean C–C = 1.39 (24, 3) Å. [c] Distances cis to a bridging sulfide. [d] Distances trans to a bridging sulfide.

dithiolene ligands, Mo–S(3 and Mo–S(5), at 2.452 and 2.466 Å, respectively, are located in the MoS(1)S(1′)S(3)S(5) plane and are trans to the shorter Mo–S(1) and Mo–S(1′) bridge bonds that have lengths of 2.319 and 2.323 Å. The short dithiolene Mo–S bonds are axial with respect to the MoS(1)S(1′)S(3)S(5) plane. The C–S bond lengths similarly can be grouped into two pairs with the shorter bonds adjacent to the long Mo–S bonds. The consequences of this apparent localization of charge on S(2) and S(4) should be propagated throughout the structure of the ligands. The observed metrical differences in the C–C and C–O bonds are consistent with such a conjugation, but they are only marginally significant. The clear evidense of a trans effect in V reenforces arguments (vide infra) that place significance in out of plane π bonding in affecting reactivity in the di-μ-S dimeric complexes. Similar differences attributable to a trans effect also are observed in the structure of the analogous W/Se complex. The Mo–Mo′ distance in V at 2.940 (2) Å is shorter than that the W–W′ distance in the W/Se analogue (2.989 (1) Å); however, it is significantly longer than the Mo–Mo distances in $[(S_2)(Mo(O)(\mu\text{-}S)_2Mo(O)(S_4)]^{2-}$ (2.828 (1) Å),[11] $[(S_2)(Mo(O)(\mu\text{-}S)_2Mo(O)(C_5H_5)]^-$ (2.855 (2) Å),[51] $[(S_2)(Mo(O)(\mu\text{-}S)_2Mo(O)(DMF)_3]$ (2.814 (2) Å),[52] II (2.903 (1) Å), and III (2.851 (1) Å). The Mo–S_b bonds in V (2.321 (3) Å are within 3σ to corresponding bonds in II, 2.327 (1) Å, and III, 2.330 (4) Å.

Mo–η^2-S_4^{2-}, Mo–η^2-S_2^{2-}, Mo=O, and Mo=S Functional Groups

An analysis of the structural and reactivity data available for the various $[(L)Mo^V_2(\mu_2\text{-}S)_2(E)_2(L')]^{n-}$ and $[(L)Mo^{IV}(E)(L')]^{n-}$ thiomolybdate complexes (E = O^{2-}, S^{2-}; L, L′ = O^{2-}, S^{2-}, S_2^{2-}, Cp^-, CS_4^{2-}, S_4^{2-}) reveals trends that can be attributed to distal

(51) Toupadakis, A.; Koo, Sang-Man; Coucouvanis, D. Manuscript in preparation.
(52) Coucouvanis, D.; Toupadakis, A.; Hadjikyriacou, A. *Inorg. Chem.* **1988**, *27*, 3272.

Table VIII. Infrared, ^{1}H NMR, and Electronic Spectral Data for $[Et_4N]_2[MoO(S_2C_2(CO_2Me)_2)_2]$ (I), *anti*-$[Et_4N]_2[Mo_2O_2S_2(S_2C_2(CO_2Me)_2)_2]$ (II), *syn*-$[Ph_4P]_2[Mo_2O_2S_2(S_2C_2(CO_2Me)_2)_2]\cdot 2DMF$ (III), $[(cis\text{-}\eta^1\text{-}S\text{-}\eta^1\text{-}CSC(CO_2Me)_2)_2\text{-}syn\text{-}\{Mo_2(O)_2(\mu\text{-}S)_2\}]^{2-}$ (IIIb), $[Ph_4P]_2[Mo(S_2C_2(CO_2Me)_2)_3]\cdot DMFC_6H_6$ (IV), $[Ph_4P]_2[Mo_2S_2(S_2C_2(CO_2Me)_2)_4]\cdot 2CH_2Cl_2$ (V), and $[(\eta^1\text{-}S\text{-}\eta^1\text{-}CSC(CO_2Me)_2)(O)Mo(\mu_2\text{-}S)_2Mo(O)(S_4)]^{2-}$ (VI)

compd	ν(Mo–O),[a] cm^{-1}	ν(Mo–S),[a] cm^{-1}	^{1}H NMR, δ	electronic data,[b] nm	CV E_p,[c] V
I	914 (s)	388 (w), 348 (w)	3.62 (s, 12 H)	360, 460 (sh), 550	−0.029 (rev),[d] +0.821 (irr)
II	923 (s), 911 (w)	462 (w)	3.703 (s, 12 H)[e] 3.759 (s, 12 H)[f]	318, 380 (sh)	+0.953 (irr), +1.112 (irr)
III	942 (m)	463 (w)	3.705 (s, 12 H)[e]		+1.016 (irr), +1.201 (irr)
III[g]	942 (m)	466 (w), 386 (vw), 359 (w), 345 (w)	3.717 (s, 12 H)[e]		
IIIb	940 (s)	469 (w), 420 (vw), 382 (w), 358 (w), 331 (w)	3.712 (s, 6 H),[e] 3.766 (s, 6 H)[e]		
IV			3.59 (s, 18 H)[h]	356, 450 (sh), 650	+0.020 (rev),[i] +0.420 (rev)
V			3.65 (s, 24 H)[h]	380, 582, 430 (sh), 680	−0.800 (qrev), +0.711 (irr)
VI	945 (vs)	462 (w), 375 (vw), 354 (vw), 337 (w), 327 (w)	3.728 (s, 3 H),[e] 3.770 (s, 3 H)[e]		

[a] Obtained in KBr disks. [b] Obtained in CH_3CN solution. [c] Obtained on a Pt electrode in CH_3CN solution vs a Ag/AgCl reference electrode; rev = reversible, qrev = quasireversible, and irr = irreversible. [d] $E_{1/2}$. [e] Signal intensity relative to the eight CH_2 protons in the Et_4N^+ cation, in DMSO-d^6 solution. [f] Signal intensity relative to the eight CH_2 protons in the Et_4N^+ cation, in CD_3CN. [g] The Et_4N^+ salt analogue of III. [h] Signal intensity relative to the forty phenyl H atoms in the Ph_4P^+ cation. [i] $E_{1/2}$ values obtained in CH_2Cl_2 solution on a Pt working electrode vs a saturated calomel electrode, SCE.

Table IX. Comparison of the Syn and Anti Isomers of the $[Mo_2O_2S_2(S_2C_2(CO_2Me)_2)_2]^{2-}$ (A)[a] and $[Mo_2S_4(S_2C_2H_4)_2]^{2-}$ (B)[b] Anions

	syn-A	*anti*-A	*syn*-B	*anti*-B
	Average Interatomic Distances (Å)			
Mo–Mo	2.853 (1)	2.904 (1)	2.863 (2)	2.878 (2)
Mo–S_b[c]	2.331 (3)	2.328 (1)	2.320 (5)	2.321 (33)
Mo=O_t (S_t)	1.675 (2)	1.684 (2)	2.101 (16)	2.129 (3)
Mo–S_t[d]	2.425 (8)	2.419 (1)	2.406 (2)	2.401 (19)
S_b–S_b[c]	3.556 (5)	3.640 (2)	3.550 (7)	3.658 (4)
	Average Bond Angles (deg)			
Mo–S_b–Mo	75.5 (1)	77.13 (1)	76.23 (7)	76.62 (7)
S_b–Mo–S_b[c]	100.9 (1)	102.91 (1)	99.85 (8)	103.38 (7)
S_t–Mo–S_t[d]	81.2 (1)	81.44 (1)	81.1 (1)	80.97 (9)
dihedral angle	156.6 (3)	180	146.9 (3)	180

[a] This work. [b] From ref 38. [c] S_b = a bridging sulfur atom. [d] S_t = a chelating ligand sulfur atom.

or proximal electronic effects associated with the axial (E) and equatorial (L, L′) ligands.

Mo–η^2-S_4^{2-} Group. In most cases the chemistry of the Mo–η^2-S_4^{2-} group can be attributed to the presence of the Mo–η^2-S_2^{2-} group[36] that emerges as the "activated" S_4^{2-} ligand dissociates S_2. Direct evidence for a Mo–η^2-S_4^{2-}/Mo–η^2-S_2^{2-} equilibrium has been obtained unequivocally by ^{1}H NMR spectroscopic studies in CH_3CN solutions of $[(Cp)(O)Mo^V(\mu\text{-}S)_2Mo^V(O)(S_2)]^-$ and elemental sulfur.[36] The activation of the coordinated S_4^{2-} ligand and the subsequent dissociation of S_2 seems to be a consequence of both distal and proximal electronic effects. In the $[(L)Mo_2(\mu_2\text{-}S)_2(E)_2(L')]^{n-}$ complexes, the π-donor ligands S_4^{2-} and Cp^- on one side of the dimeric complexes can affect the reactivity of the ligands on the opposite side. This is illustrated in the ready dissociation of S_2 from the $[(S_4)Mo_2(\mu_2\text{-}S)_2(E)_2(S_4)]^{2-}$ and $[(S_4)Mo_2(\mu_2\text{-}S)_2(O)_2(Cp)]^-$ complexes.[36] Similarly, dissociation of CS_2 readily occurs in analogous complexes where the S_4^{2-} ligands have been replaced by CS_4^{2-}.[53] In contrast no dissociation of S_2 is observed in solutions of the $[(S_4)Mo_2(\mu_2\text{-}S)_2(E)_2(S_2)]^{2-}$ complexes where the η^2-S_2^{2-} ligand, a weaker π donor, is not affecting the distant S_4^{2-} ligand. The propagation of electronic effects across the length of these molecules could be rationalized in terms of extensive delocalization of electron density within the "out of plane" π system that involves the d_{xz} and d_{yz} orbitals on the Mo^V atoms and "out of plane" p orbitals on the sulfur ligands. As a consequence of these effects, conversion of a η^2-S_2^{2-} ligand in the $[(S_2)Mo_2(\mu_2\text{-}S)_2(E)_2(S_4)]^{2-}$ complexes to dithiolene, vinyl disulfide, or CS_4^{2-} promotes the dissociation of S_2 from the distant S_4 ligand with generation of another η^2-S_2^{2-} ligand that further reacts with electrophilic reagents.

Proximal effects also are important in the activation of the coordinated η^2-S_4^{2-} and η^2-CS_4^{2-} ligands in the $[(L)Mo_2(\mu_2\text{-}S)_2(E)_2(L)]^{2-}$ complexes (L = CS_4^{2-}, S_4^{2-}). In general, η^2-S_4^{2-} ligands proximal to oxo axial ligands do not dissociate S_2 readily and are less reactive than those proximal to sulfido axial ligands. The p orbitals of the axial E groups (E = O, S) overlap and form two π bonds with the Mo d_{xz} and d_{yz} orbitals that also have the proper symmetry to π bond with the 3p orbitals of the S donor atoms in equatorial L, L′ ligands. The strongly electron-withdrawing oxo group apparently is more effective than a terminal sulfido group in weakening the Mo–S (out of plane) π bonding and indirectly strengthens the pπ–pπ interactions in the S–S bonds directly adjacent to the Mo–S bonds. Crystallographic data, available for the $[(S_4)_2Mo{=}E]^{2-}$ complexes,[3] marginally support the previous arguments regarding the effects of neighboring axial ligands. The S–S bonds proximal to the Mo–S bonds in the $(O)Mo(S_4)$ unit (S–S = 2.083 Å) are slightly shorter than those in the $(S)Mo(S_4)$ units (S–S = 2.090 Å). The opposite is observed with the Mo–S bonds that are slightly shorter in the $(S)Mo(S_4)$ units (Mo–S = 2.359 Å) than those in the $(O)Mo(S_4)$ units (Mo–S = 2.379 Å).

In the $[(S_4)Mo_2(\mu_2\text{-}S)_2(E)_2(S_2)]^{2-}$ complexes,[3,11] the easily polarizable η^2-S_2^{2-} ligands also react readily with nucleophiles such as trialkyl- or triarylphosphines and are more reactive than the η^2-S_4^{2-} ligands. The abstraction of S with Ph_3P, from the $(S_2)Mo{=}S$ and $(S_2)Mo{=}O$ units in these complexes, occurs at ambient temperature and results in the formation of the $[(S_4)Mo(E)(MoS_3E)]^{2-}$ complexes.[1,54] The η^2-S_4^{2-} ligands do not react further with Ph_3P unless heated to 80 °C for extended periods of time.

Mo=S and Mo=O Groups. In addition to reactions with the Mo–η^2-S_2^{2-} units, the formation of different products in reactions of the $[(S_x)Mo^V_2(\mu_2\text{-}S)_2(E)_2(S_x)]^{2-}$ (x = 2, 4) and $[(S_4)_2Mo^{IV}(E)]^{2-}$ complexes (E = S vs E = O) with DMA directly or indirectly are due to the Mo=S and Mo=O groups. Thus, while the Mo=O unit appears rather unreactive toward electrophilic reagents, the Mo=S unit readily undergoes electrophilic attack by DMA. It is apparent that in thiomolybdates that contain both Mo=S and Mo(η^2-S_x) groups, reactions with DMA proceed until all nonbridging S_x^{2-} ligands (x = 1, 2, 4) are converted into the dithiolene (DMAD) ligands. This is aptly illustrated in the syntheses of IV and V in reactions of the $[(L)Mo^V_2(\mu_2\text{-}S)_2(S)_2(L)]^{2-}$ (L = CS_4; L = S_x, x = 2, 4) and $[(S_4)_2Mo^{IV}(S)]^{2-}$ complexes with DMA (Figure 9). The most likely initial step, which follows the electrophilic attack by DMA, is insertion either into

(53) Draganjac, M. Ph.D. Thesis, University of Iowa, 1983.

(54) Toupadakis, A. Ph.D. Thesis, University of Michigan, 1990.

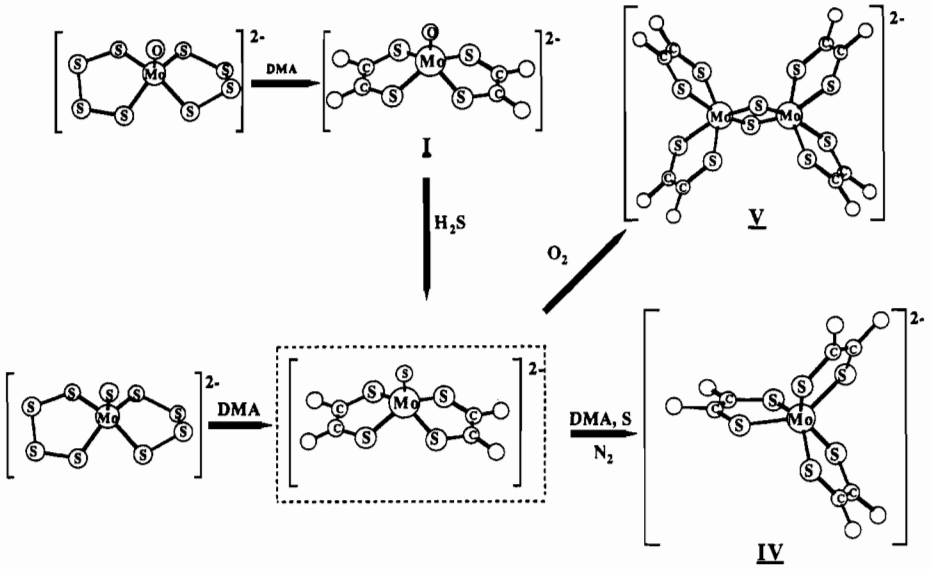

Figure 9. Possible reaction pathways in the syntheses of $[Mo(S_2C_2(CO_2Me)_2)_3]^{2-}$ (IV) and $[Mo_2S_2(S_2C_2(CO_2Me)_2)_4]^{2-}$ (V).

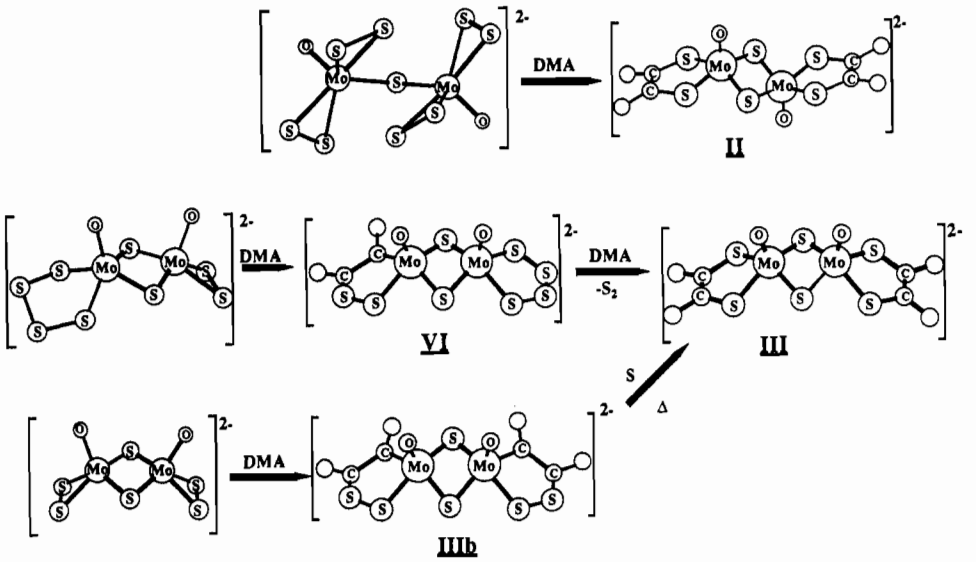

Figure 10. Syntheses of *anti*-$[Mo_2O_2S_2(S_2C_2(CO_2Me)_2)_2]^{2-}$ (II) and *syn*-$[Mo_2O_2S_2(S_2C_2(CO_2Me)_2)_2]^{2-}$ (III).

the Mo=S bond with formation of vinyl sulfide or into the Mo–η^2-S_2 bond with formation of vinyl disulfide (Figure 10). Insertion of sulfur (always present in solution as a result of $(L)MoS_4^{2-} \rightleftharpoons (L)MoS_2^{2-}$ equilibria[36]) into the Mo–C bond of the vinyl sufide intermediate or a sulfur-catalyzed isomerization of the vinyl disulfide complex is expected to produce the dithiolene ligands in II and III. The formation of the coordinated vinyl sulfide ligand (η^1-S-η^1-$CSC(CO_2Me)_2$) has been observed directly by ^1H NMR spectroscopy in the reaction of the $[(Cp)(O)Mo^V(\mu_2\text{-}S)_2Mo^V(O)(\eta^1\text{-}S\text{-}\eta^1\text{-}CSC(CO_2Me)_2)]^-$ complex with Ph_3P.[36] The vinyl sulfide complex readily inserts sulfur into either the Mo–C or the Mo–S bonds of the coordinated vinyl sulfide ligand to give vinyl disulfide or dithiolene, respectively. Additional evidence for the formation of vinyl sulfide species, which follows insertion of DMA into the Mo=S bond, is provided by reactivity studies of the $[(S_4)Mo_2(\mu_2\text{-}S)_2(O)_2(S)]^{2-}$ complex. This complex is obtained by Ph_3P sulfur abstraction from the $[(S_4)Mo_2(\mu_2\text{-}S)_2(O)_2(S_2)]^{2-}$ complex, and its structure has been determined.[55] Its reaction with 1 equiv of DMA was monitored by ^1H NMR spectroscopy in CD_3CN. The spectrum initially shows two carbomethoxy group methyl resonances (at 3.826 and 3.743 ppm) that are tentatively assigned to a vinyl sulfide ligand. These resonances are different from those observed for VI in the same solvent (Table I).

A possible reaction pathway for the synthesis of IV and V from $[(S_4)_2Mo^{IV}(S)]^{2-}$ is shown in Figure 9. Some support for the proposed $[(L)_2Mo^{IV}(S)]^{2-}$ (L = η^1-S-η^1-$CSC(CO_2Me)_2$, η^1-S-η^1-$SC_2(CO_2Me)_2$) common precursor to IV and V is provided by the reaction of I with H_2S. This reaction converts the Mo=O group in I to Mo=S, and the product subsequently dimerizes to give V.

In the absence of excess sulfur, vinyl sulfide intermediates not only abstract sulfur intermolecularly to eventually form dithiolenes but also may undergo self-condensation that leads to polymerization. Indeed, reactions of DMA with thiomolybdates that do not contain S_2^{2-} or S_4^{2-} terminal ligands such as $[Mo_2S_6]^{2-}$, and in the absence of elemental sulfur, invariably lead only to polymeric ill-defined materials.[54]

Thus far, intermediates containing the vinyl sulfide or vinyl disulfide chelating ligands have not been detected in reactions of DMA with complexes that contain exclusively sulfur ligands. Apparently, the close proximity of Mo=S, Mo–S_2^{2-}, or Mo–S_4^{2-} groups to the reactive vinyl sulfide or disulfide ligands in these intermediates allows for rapid intramolecular sulfur transfer and rapid conversion to dithiolenes. The detection or isolation of vinyl sulfide or vinyl disulfide intermediates, in complexes where reactive =S or η^2-S_2^{2-} groups are proximal to =O on the same Mo atom,

(55) Koo, Sang-Man; Toupadakis, A.; Coucouvanis, D. Manuscript in preparation.
(56) Johnson, C. K. *ORTEP*; Report ORNL-3794; Oak Ridge National Laboratory: Oak Ridge, TN, 1965.

is possible (Figure 10) because in such complexes intramolecular S transfer following DMA insertion reactions cannot occur. This accounts for the stability and isolation of the cis-syn vinyl disulfide precursor of III (Figure 10; IIIb). The X-ray crystal structure of the latter has been reported.[30]

Additional support for the proposed vinyl disulfide intermediates in DMA insertion reactions is provided by detailed ^{1}H NMR studies of the reaction of the $[(Cp)(O)Mo^V(\mu\text{-}S)_2Mo^V(O)(S_2)]^-$ complex with DMA.[36] These reactions demonstrate that insertion into the coordinated S_2^{2-} ligand and formation of vinyl disulfide precedes the final formation of dithiolene. At elevated temperatures (~70 °C), in CH_3CN solution, the coordinated vinyl disulfide slowly converts to dithiolene. This conversion is rapid in the presence of catalytic amounts of elemental sulfur. Possible pathways for these transformations have been proposed previously.[36]

A similar pathway, involving vinyl disulfide intermediates, most likely is followed in reactions that lead to the synthesis of II and III (Figure 10). A particular pathway for the formation of I from the reaction of $[(S_4)_2Mo^{IV}(O)]^{2-}$ with DMA is not clear. It has not been possible to detect evidence for the dissociation of S_2 from the $[(S_4)_2Mo^{IV}(O)]^{2-}$ anion or for the presence of vinyl disulfide intermediates in the course of the reaction. At this stage other possible mechanisms such as cycloaddition to the coordinated S_4 ligand followed by elimination of S_2 cannot be ruled out.

Acknowledgment. The financial support of this project by the National Science Foundation is gratefully acknowledged. The assistance of Dr. J. Seela with some of the electrochemical measurements also is acknowledged.

Supplementary Material Available: For I-III and V, Tables S1-S4, listing hydrogen coordinates, thermal parameters for all atoms, and detailed bond distances and angles (45 pages); listings of calculated and observed structure factors (52 pages). Ordering information is given on any current masthead page. The corresponding data for IV already have been deposited with the preliminary communication reporting on the structure of IV[24] and also can be found in ref 53.

Contribution from the Department of Chemistry and Laboratory for Molecular Structure and Bonding, Texas A&M University, College Station, Texas 77843

Solution and Solid-State Conformational Isomers of the Molecular Dihydrogen Complex $ReCl(H_2)(PMePh_2)_4$: Does It Contain an Asymmetric Molecular Dihydrogen Ligand?

F. Albert Cotton* and Rudy L. Luck

Received August 3, 1990

The complex $ReCl(H_2)(PMePh_2)_4$ with four $PMePh_2$ ligands in the equatorial plane and the Cl^- ligand trans to an η^2-H_2 ligand has been investigated by means of variable-temperature ^{1}H and $^{31}P\{^1H\}$ NMR spectroscopies in different solvents, namely, CD_2Cl_2, acetone-d_6, and toluene-d_8. In this crowded molecule metastable conformational isomers based on rotational orientations about the Re-P bonds can arise. The data obtained indicate that different percentages of conformational isomers are formed in the different solvents. The T_1(min) time of 92 ms at 400 MHz in CD_2Cl_2 is obtained for the metal-bonded H atoms in $ReCl(H_2)(PMePh_2)_4$. Structural data are reported for $ReCl(H_2)(PMePh_2)_4\cdot 2C_4H_8O$ (**1a**) at 292 and 193 K, $ReCl(H_2)(PMePh_2)_4\cdot 0.5(CH_3)_2CO$ (**1b**), and $ReCl(H_2)(PMePh_2)_4\cdot 0.5(CH_3)_2CO$ (**1c**). These different crystalline forms were obtained under different crystallization conditions. Crystal data: compound **1a**, triclinic, space group $P\bar{1}$, a = 12.287 (3) Å, b = 19.318 (8) Å, c = 12.275 (3) Å, α = 101.06 (3)°, β = 104.42 (2)°, γ = 103.83 (3)°, V = 2640 (4) Å^3, Z = 2, T = 292 K, R = 0.055 (R_w = 0.073) for 446 parameters and 5091 unique data having $F_o > 3\sigma(F_o)^2$; compound **1a**, triclinic, space group $P\bar{1}$, a = 12.210 (4) Å, b = 19.269 (9) Å, c = 12.138 (4) Å, α = 101.10 (3)°, β = 103.92 (2)°, γ = 104.13 (3)°, V = 2590 (4) Å^3, Z = 2, T = 193 K, R = 0.041 (R_w = 0.058) for 449 parameters and 7334 unique data having $F_o > 3\sigma(F_o)^2$; compound **1b**, triclinic, space group $P\bar{1}$, a = 13.044 (3) Å, b = 18.434 (5) Å, c = 11.701 (4) Å, α = 94.12 (3)°, β = 113.44 (2)°, γ = 80.58 (2)°, V = 2547 (2) Å^3, Z = 2, T = 292 K, R = 0.046 (R_w = 0.063) for 467 parameters and 6089 unique data having $F_o > 3\sigma(F_o)^2$; compound **1c**, triclinic, space group $P\bar{1}$, a = 14.186 (4) Å, b = 17.317 (4) Å, c = 11.675 (3) Å, α = 108.57 (2)°, β = 96.32 (2)°, γ = 76.39 (2)°, V = 2640 (2) Å^3, Z = 2, T = 292 K, R = 0.036 (R_w = 0.067) for 487 parameters and 8763 unique data having $F_o > 3\sigma(F_o)^2$. In forms **1a** and **1b** the main molecule was ordered and the final difference maps revealed two electron density maxima near the Re atom and trans to the Cl^- ligand that could be representative of two H atoms bonded to the Re atom in an η^1-H_2 mode. For both data sets with form **1a** these H atoms failed to refine freely to reasonable parameters. However, the positions of these atoms from the difference maps are reported. In form **1b** the two H atoms were refined freely, which resulted in the following parameters: Re-H(1) = 1.49 (9) Å, Re-H(2) = 1.98 (9) Å, H(1)-H(2) = 1.17 (13) Å, Re-H(1)-H(2) = 95 (8)°, and Re-H(2)-H(1) = 48 (6)°. Form **1c** contains disorder between the trans Cl^- and η-H_2 ligands.

Introduction

Since the important discovery by Kubas[1] that the complex $W(\eta^2\text{-}H_2)(CO)_3(PCy_3)_2$, Cy = cyclohexyl, contains a molecular dihydrogen ligand, many other such complexes have been synthesized[2-15] and previously known complexes containing polyhydride ligands have been reassigned as containing molecular dihydrogen ligands.[16] Some of these latter reassignments have been based exclusively on the ^{1}H NMR longitudinal relaxation time (T_1)[16b] and we have since then pointed out several difficulties associated with this technique.[17] More recently, additional refinements to the interpretation of the T_1 results have been suggested.[18]

Previous structural results[8b,10,11b,12a,c] on the nature of the η^2-H_2 ligand have established so far a symmetrical arrangement with equal (within esd's) M-H distances. Theoretical calculations[19] do suggest that the symmetrical bonding mode η^2-H_2 (I) is

I II

* To whom correspondence should be addressed.

(1) Kubas, G. J. *Acc. Chem. Res.* **1988**, *21*, 120 and references therein.
(2) Bianchini, C.; Mealli, C.; Meli, A.; Peruzzini, M.; Zanobini, F. *J. Am. Chem. Soc.* **1988**, *110*, 8725.
(3) (a) Albertin, G.; Antoniutti, S.; Bordignon, E. *J. Am. Chem. Soc.* **1989**, *111*, 2072. (b) Amendola, P.; Antoniutti, S.; Albertin, G.; Bordignon, E. *Inorg. Chem.* **1990**, *29*, 318.
(4) Collman, J. P.; Wagenknecht, P. S.; Hembre, R. T.; Lewis, N. S. *J. Am. Chem. Soc.* **1990**, *112*, 1294.
(5) (a) Cotton, F. A.; Luck, R. L. *J. Chem. Soc., Chem. Commun.* **1988**, 1277. (b) Cotton, F. A.; Luck, R. L. *Inorg. Chem.* **1989**, *28*, 2181.
(6) Luo, X.-L.; Crabtree, R. H. *J. Chem. Soc., Chem. Commun.* **1990**, 189.
(7) Chinn, M. S.; Heinekey, D. M. *J. Am. Chem. Soc.* **1990**, *112*, 5166.

0020-1669/91/1330-0767$02.50/0